DOE/ER/14208--1-Pt.2

CONF-9111114--2-Pt.2

Geosciences Research Program ER-15

OFFICE OF BASIC ENERGY SCIENCES

Field Trip Guide to Selected Outcrops, Arbuckle Mountains, Oklahoma

in conjunction with Sedimentary Basin Geochemistry and Fluid/Rock Interactions Workshop

November 17, 1991

Field Trip Leaders

Brian Cardott, Oklahoma Geological Survey
R. Douglas Elmore, School of Geology and Geophysics

School of Geology and Geophysics

THE UNIVERSITY OF OKLAHOMA

DISCLAIMER

Arbuckle Mountain Field Trip

Introduction

The Arbuckle Mountains, named for Brigadier General Matthew Arbuckle, are located in south-central Oklahoma. The formations that comprise the Arbuckle Mountains have been extensively studied for hydrocarbon source rock and reservoir rock characteristics that can be applied to the subsurface in the adjacent Anadarko and Ardmore basins.

Numerous reports and guidebooks have been written concerning the Arbuckle Mountains. A few important general publications are provided in the list of selected references. The most detailed report on the regional geology of the Arbuckle Mountains is by Ham (1973).

The purpose of this handout is to provide general information on the geology of the Arbuckle Mountains and specific information on the four field trip stops, adapted from the literature.

General Geology

The following description of the geology and significance of the Arbuckle Mountains is adapted from Johnson and others (1984), which was slightly modified from Ham (1969).

The geological province known as the Arbuckle Mountains consists of a huge inlier of folded and faulted Paleozoic and Precambrian rocks. It is covered on the east, north, and west by gently westward-dipping Pennsylvanian and Permian strata and on the south by gently southward-dipping Cretaceous sediments of the Gulf Coastal Plain (Fig. 1).

The primary emphasis of Arbuckle Mountains geology lies in its early Paleozoic carbonates and late Paleozoic clastics (sandstones and shales), deposited partly upon a craton of Precambrian igneous rocks and partly in a geosyncline (southern Oklahoma aulacogen, SOA) in which the basement rocks are Cambrian rhyolites. The stable craton extends from the eastern Arbuckle Mountains granite outcrops northward through central Oklahoma into Kansas and beyond. At a fault-zone contact (Washita Valley Fault zone) these rocks are separated from the southwestern segment of the Arbuckle Mountains, known as the Arbuckle Anticline, where the depositional history is that of the geosyncline (SOA). The geosyncline includes the Arbuckle Anticline and extends southward for about 50 miles (80 km), across the Ardmore basin and Marietta basin, and terminates in the subsurface of north Texas against the Precambrian cratonic rocks of that state. Westward, the geosyncline (SOA) includes the Anadarko basin.

The Arbuckle Anticline is the most intensely deformed part of the mountains. Structurally it is a faulted anticline, overturned to the north (Fig. 2). Within the faulted area is a graben containing remnants of the Pennsylvanian-aged Collings Ranch Conglomerate. The conglomerate is faulted and warped into a synclinal fold, indicating that deformation continued during and after deposition of the Collings Ranch

STRATIGRAPHIC SECTION EXPOSED ON I-35 THROUGH THE ARBUCKLE ANTICLINE AND MAPPED AREA

SYSTEM	GROUP, FORMATION AND MEMBER	MAP SYMBOL	THICKNESS (ft) SOUTH FLANK	NORTH FLANK
QUATERNARY	Alluvium and Terrace deposits	Qat		
	UNCONFORMITY			
PERMIAN – PENNSYLVANIAN	Pontotoc Group *undifferentiated*	Po/IPp		
	UNCONFORMITY			
PENNSYLVANIAN	Collings Ranch Conglomerate	IPcr		3000 estimated
	UNCONFORMITY			
MISSISSIPPIAN	Goddard Shale	Mg	2500	
	Delaware Creek Shale (formerly "Caney" Shale)	Md	425	
	Sycamore Limestone	Ms	358	221
DEVONIAN	Woodford Shale	MDw	290	274
	Hunton Group (DSOh): Bois d'Arc Limestone	*	9	19
	Hunton Group (DSOh): Haragan Formation	*	25	16
SILURIAN	Henryhouse Formation	*	191	72
	Chimneyhill Subgroup: Clarita Limestone	*	12	16
	Chimneyhill Subgroup: Cochrane Limestone	*	13	4+
ORDOVICIAN	Chimneyhill Subgroup: Keel Limestone	*		7
	Sylvan Shale	Os	305	275
	Viola Group	Ov	684	710
	Simpson Group: Bromide Formation	Obr	420	346
	Simpson Group: Poolville Limestone Member	*	120	80
	Simpson Group: Mountain Lake Member	*	300	266
	Simpson Group: Tulip Creek Formation	Otc	395	297
	Simpson Group: McLish Formation	Oml	475	397
	Simpson Group: Oil Creek Formation	Ooc	747	
	Simpson Group: Joins Formation	Oj	294	
	Upper Arbuckle Gp: West Spring Creek Formation	Ow	1515	
	Upper Arbuckle Gp: Kindblade Formation	Ok	1410	
	Upper Arbuckle Gp: Cool Creek Formation	Occ	1300	
	Upper Arbuckle Gp: McKenzie Hill Formation	Omh	900	
	Upper Arbuckle Gp: Butterly Dolomite	Ob	297	
CAMBRIAN	Lower Arbuckle Group: Signal Mountain Formation	€sm	415	
	Lower Arbuckle Group: Royer Dolomite	€ry	717	
	Lower Arbuckle Group: Fort Sill Limestone	€fs	155	
	Timbered Hills Group: Honey Creek Limestone	€hc	105	
	Timbered Hills Group: Reagan Sandstone	€r	240	
	Colbert Rhyolite	€c	4500 drilled	7500 estimated

★ Formation or member shown only on cross section

Source: Fay (1989)

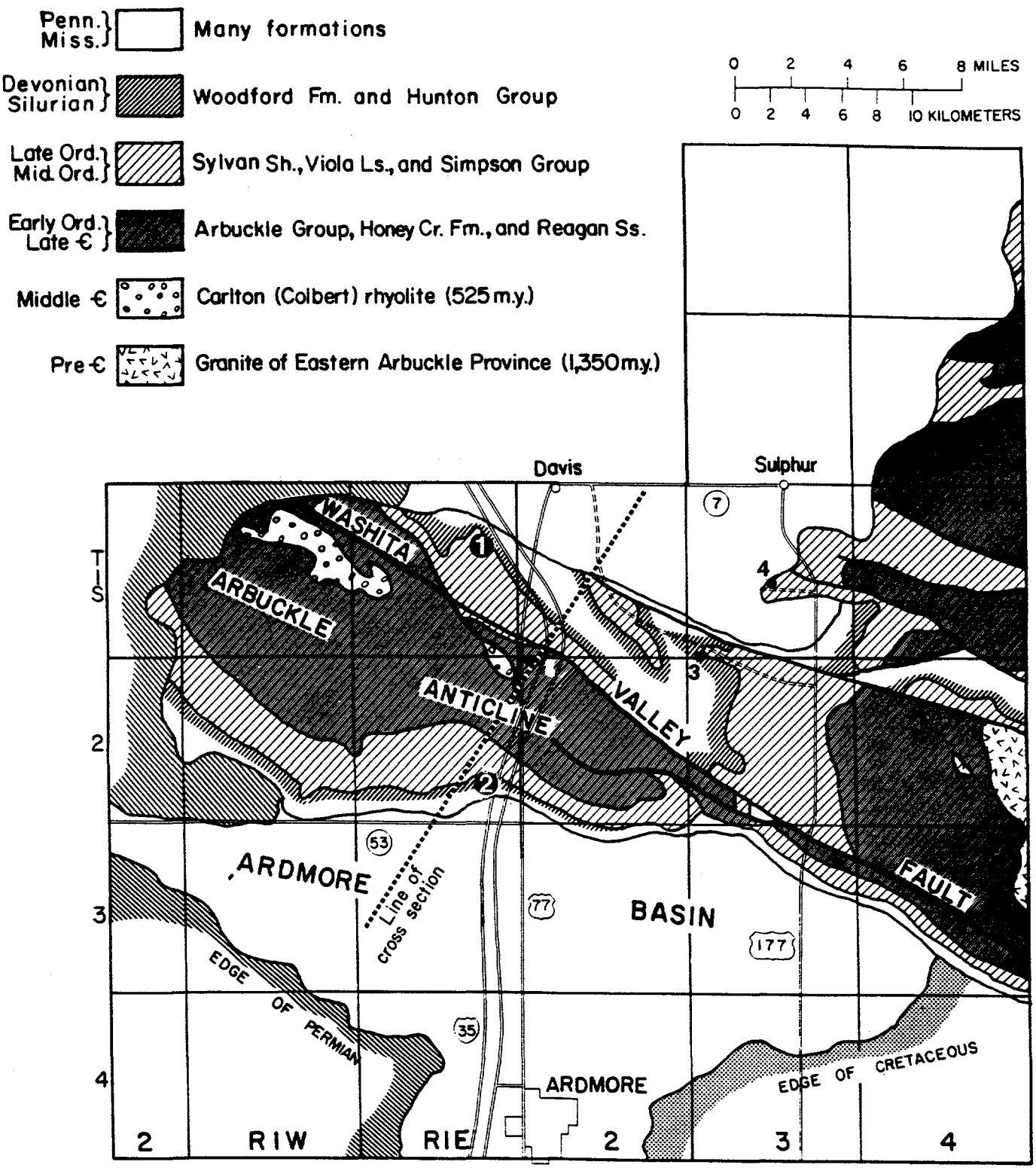

Figure 1. Generalized geologic map of Arbuckle Mountains (modified from Ham, 1969), showing location of four field-trip stops. Cross section is shown in figure 2

Adapted after Johnson and others (1984).

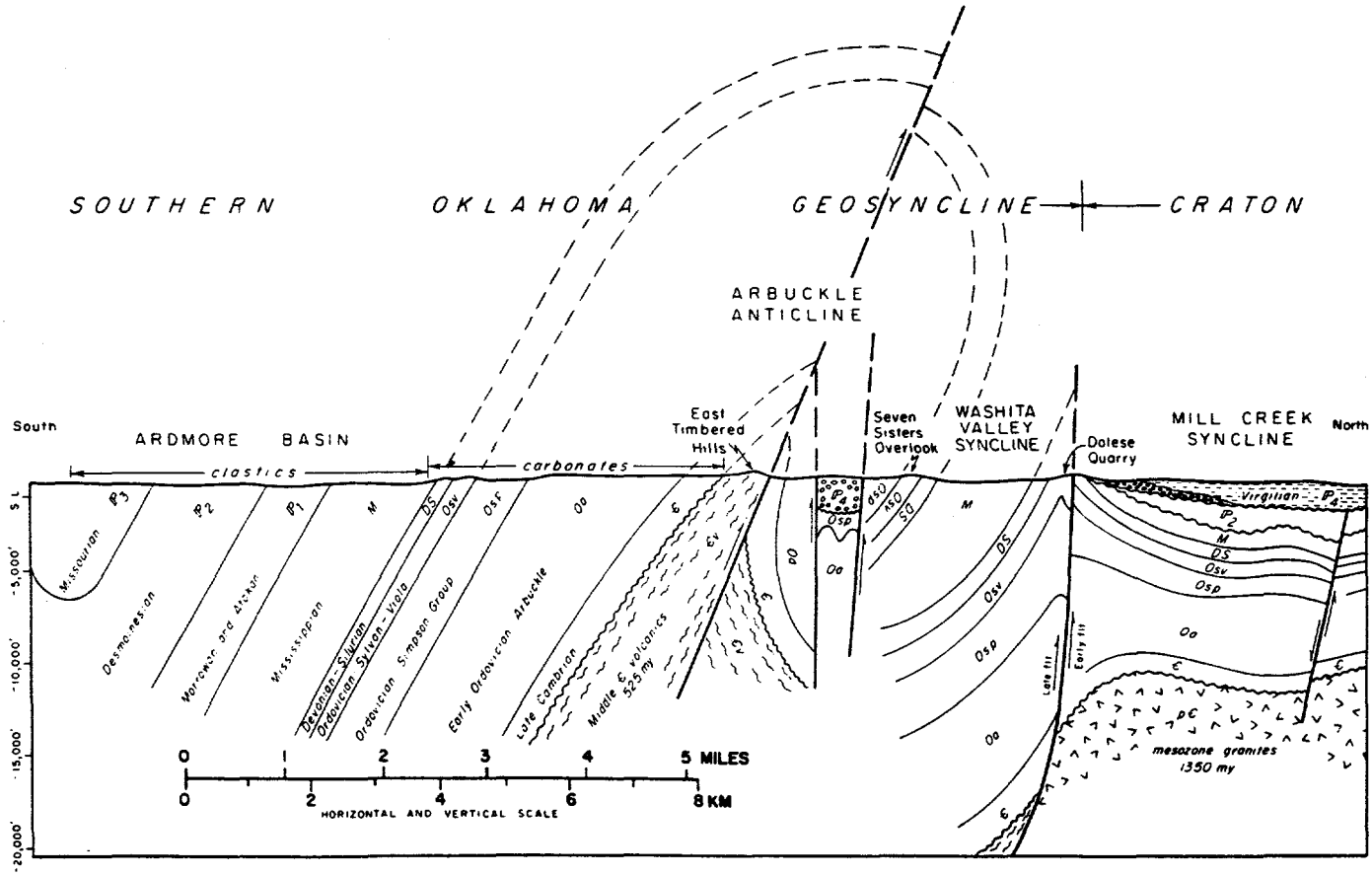

Figure **2** Structural cross section of Arbuckle Mountains in vicinity of Interstate 35 (modified from Ham, 1969). Location of cross section shown in figure **1**.

Source: Johnson and others (1984).

Conglomerate. The cross section (Fig. 2) shows the general thicknesses of geologic units and the attitudes of strata along the field-trip route.

Whether plains or hill country, the Arbuckle Mountains region is of irresistible interest to geologists, and particularly to petroleum geologists. The 11,000 ft (3,300 m) of fossiliferous Late Cambrian through Devonian strata constitute the best outcrops and greatest area of exposure of this sequence in all the Midcontinent region. Stratigraphic names taken from the Arbuckles, such as Arbuckle, Simpson, Viola, Sylvan, Hunton, and Woodford, have been widely applied in the subsurface as far away as west Texas, Illinois, and Nebraska. And these widespread rock units are among the most prolific oil- and gas-producing formations throughout the Midcontinent. Therefore, petroleum geologists have conducted extensive field investigations of the excellent exposures here in the Arbuckle Mountains.

Stop 1: Sooner Rock and Sand Quarry (secs. 11 and 14, T. 1 S., R. 1 E.). Refer to paper by Bagley and others (preprint) for a discussion of data from this quarry.

Stop 2: Woodford Shale (Late Devonian-Early Mississippian)(sec. 25, T. 2 S., R. 1 E.). South flank of the Arbuckle Mountains, west side of I-35.

The Woodford Shale is considered to be one of the most important hydrocarbon source rocks in Oklahoma (Comer and Hinch, 1987; Cardott, 1989). Cardott and others (1990, reprint attached) indicated that the Woodford Shale in the Arbuckle Mountains is immature to marginally mature with respect to the generation of oil.

Milepost 44 on figure 3 shows the approximate location of stop 2, where the Woodford Shale is designated as 'Dw'. Figure 4 illustrates a measured section taken at stop 2 by Brown and others (1985). Fay (1989) reported the thickness of the Woodford Shale at stop 2 to be 290 ft (88 m). Refer to paper by Roberts and Mitterer (preprint) for discussion of shale/chert cyclicity and geochemistry of the Woodford Shale at this location.

The type locality of the Woodford Shale is approximately eight miles west of this exposure, approximately 1/4 mile north of the town of Woodford. Lewan (1985, 1987) used Woodford Shale samples from this exposure for hydrous-pyrolysis experiments. Lewan (1983) characterized the visual-kerogen composition as being composed of 90 vol. % of amorphous Type II kerogen, with the remainder being comprised of Type III kerogen and palyniferous Type I kerogen (Tasmanites). A research subcommittee of The Society for Organic Petrology (TSOP, 1989) used Woodford Shale samples from this exposure. The results from eight laboratories indicated that the samples contained 90-95% amorphous kerogen and had 5-9% total organic carbon content (whole-rock basis). Urban (1960) and Von Almen (1970) described the palynology of the Woodford Shale from other locations in the Arbuckle Mountains.

Stop 3: Hunton Anticline and Hunton Quarry. Hunton limestone quarry; Woodford Shale Pit (sec. 31, T. 1 S., R. 3 E.).

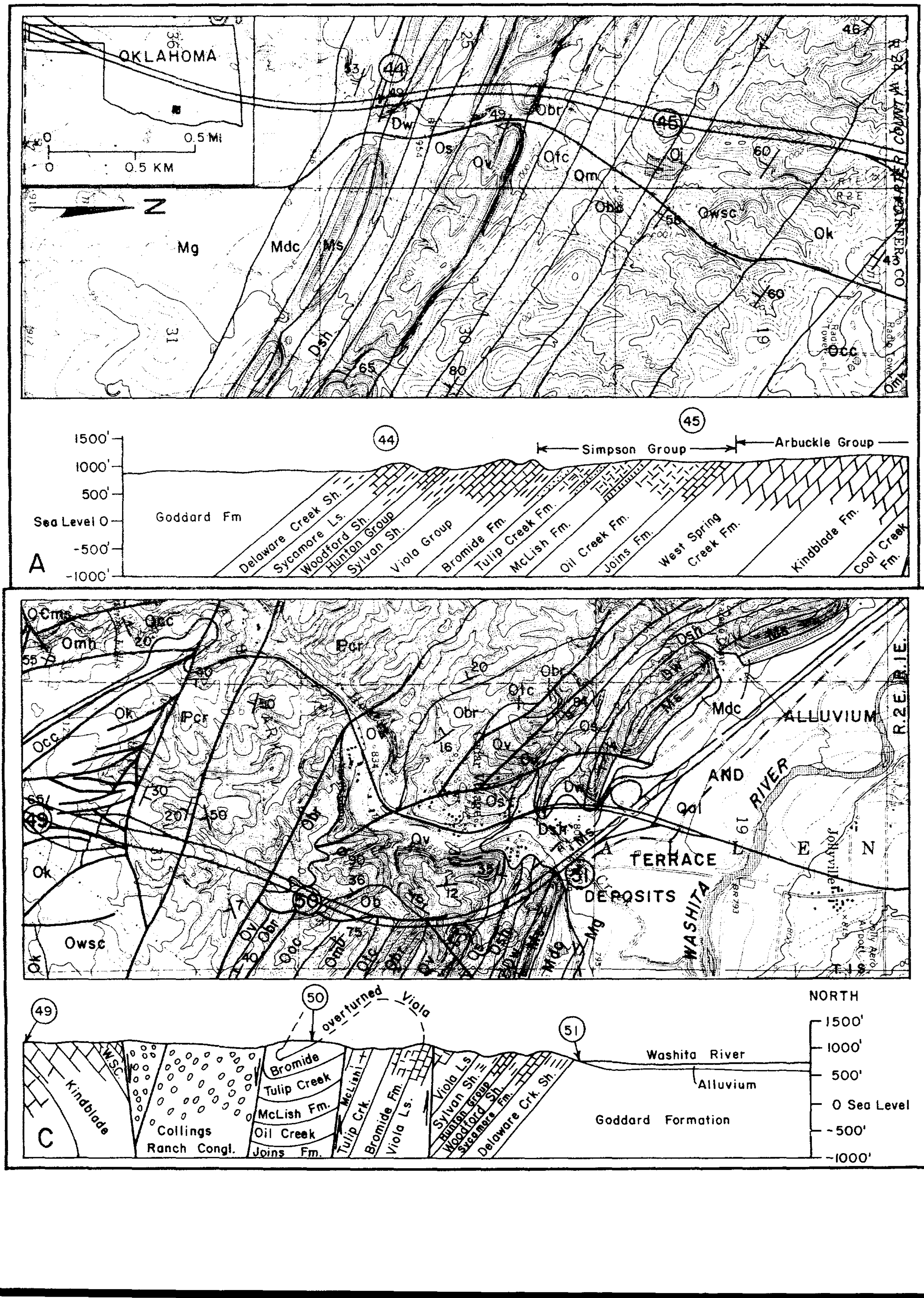
OKLAHOMA
0 0.5 Mi
0 0.5 KM
N
44
45
Dw
Os
Ov
Ofc
Obr
Om
Oj
Owsc
Ok
Occ
Mg
Mdc
Ms
Dsh
R.1 W.
R.2 W.
CARTER CO
1500'
1000'
500'
Sea Level 0
-500'
-1000'
A
Simpson Group
Arbuckle Group
Goddard Fm
Delaware Creek Sh.
Sycamore Ls.
Woodford Sh.
Hunton Group
Sylvan Sh.
Viola Group
Bromide Fm.
Tulip Creek Fm.
McLish Fm.
Oil Creek Fm.
Joins Fm.
West Spring Creek Fm.
Kindblade Fm.
Cool Creek Fm.
49
50
51
Pcr
Omb
Qal
ALLUVIUM
AND
RIVER
TERRACE
DEPOSITS
WASHITA
A L L E N
R.2E. R.1E.
NORTH
overturned Viola
Kindblade
W.S.C.
Collings Ranch Congl.
Bromide
Tulip Creek
McLish Fm.
Oil Creek
Joins Fm.
McLish
Tulip Crk.
Bromide Fm.
Viola Ls.
Sylvan Sh.
Hunton Group
Woodford Sh.
Sycamore Fm.
Delaware Crk. Sh.
Washita River
Alluvium
Goddard Formation
1500'
1000'
500'
0 Sea Level
-500'
-1000'
C

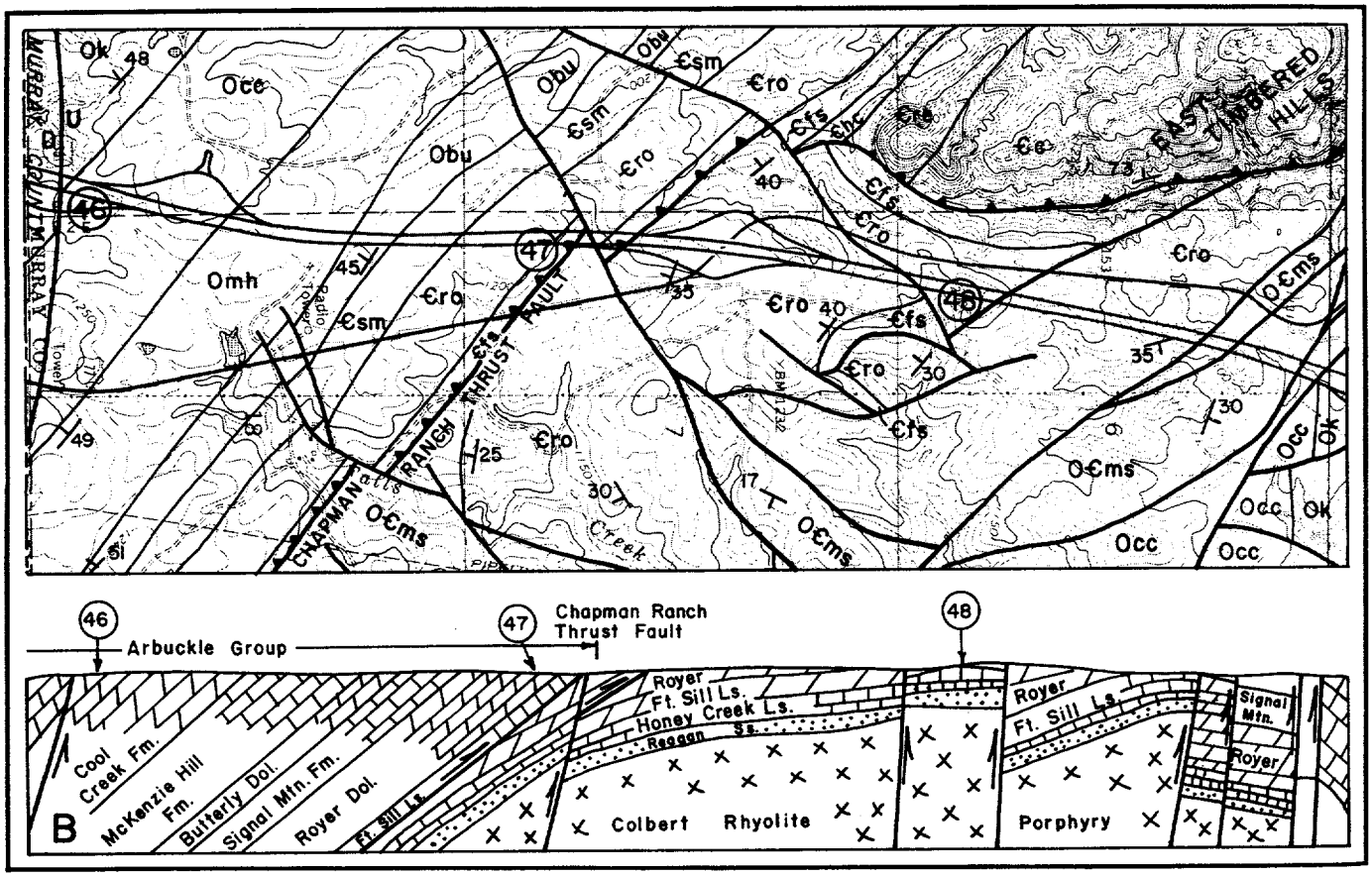

Figure 3 (this and previous page). Geologic map and profile of Arbuckle Mountains along I-35, south-central Oklahoma. A is to the south; C is to the north.

Source: Fay (1988)

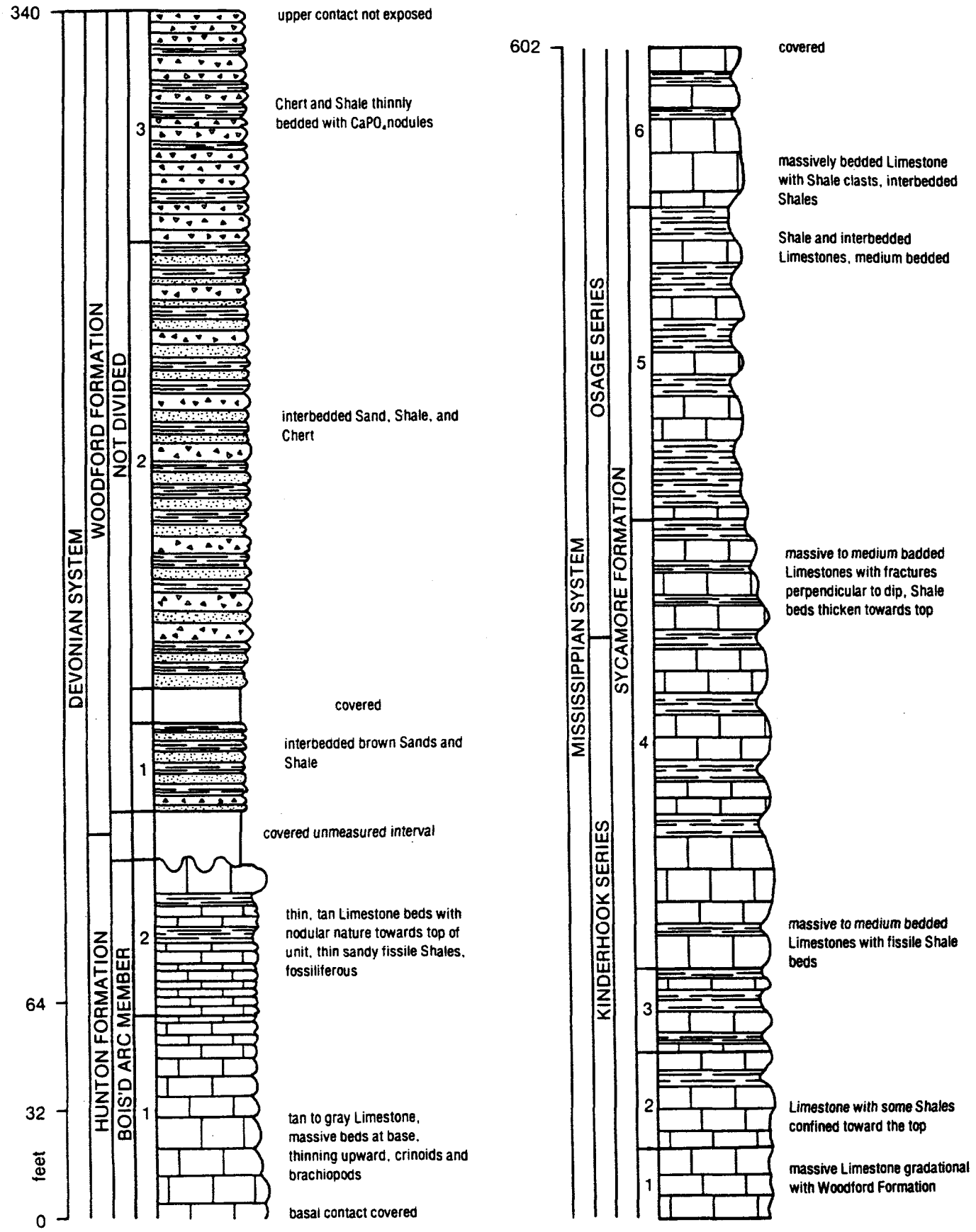

Fig. 4. Measured section of stop 2 of the Hunton, Woodford and Sycamore Formations of Silurian, Devonian and Mississippian age.
Source: Brown and others (1985).

The following summary of the Hunton quarry is modified from Johnson and others (1984).

At this stop is an excellent exposure of a plunging anticline formed in the Hunton Group limestones of Silurian and Devonian age (Fig. 5). In particular, the stone quarried is at the top of the Hunton (Fig. 6) and includes the Haragan-Bois d'Arc Formations of Early Devonian age (about 400 million years ago). Strata dip about 20° on both flanks of the anticline, and the axis of the anticline plunges toward the west-northwest at an angle of about 15° to 20°.

A single fault (thrust fault) cuts diagonally across the south limb of the anticline. The thrust dips about 30° toward the south, has a throw of about 30 ft (10 m), and passes through the axis of the fold at the top of the quarry face (Fig. 7). Compressive forces from the south caused the fold, and probably at a late stage of this folding the south block was thrust northward over the north block. This type of compression, folding, and thrusting is a small-scale representation of the movements that influenced the main Arbuckle Anticline.

Limestone has been quarried from this site and used as riprap in building the Lake of the Arbuckles dam just 0.5 mile (0.8 km) north of the quarry. Also being mined at this site is the Woodford Shale for use as base material for county roads in the area.

Stop 4: Tar Sands of Sulphur Area (sec. 15, T. 1 S., R. 3 E.).

Bitumen-impregnated sandstones and limestones occur throughout the Arbuckle Mountains area (Jordan, 1964). A number of papers and guidebooks have described these occurrences (refer to selected references list). Four major areas, in particular, were extensively quarried as sources of road-paving material until 1960. The Sulphur district (sections 15, 21, and 22, T. 1 S., R. 3 E.) contains bitumen within the sandstone member of the Oil Creek Formation (Ordovician). The Buckhorn pit (section 23, T. 1 S., R. 3 E.) contains bitumen in limestones of the Deese Group (Middle Desmoinesian). The Dougherty district (section 25, T 1 S., R. 2 E., and section 30, T. 1 S., R. 3 E.) contains bitumen in the Viola Limestone (Ordovician). The South Woodford Asphalt pit (section 12, T. 3 S., R. 1 W.) contains bitumen in the Rod Club sandstone (Upper Mississippian).

The following information about the Sulphur district was adapted from Johnson and others (1984).

The Sulphur area has been worked since about 1890 and has yielded at least 1.5 million short tons of bitumen-bearing sandstone (Fig. 8). Most of the bitumen occurs in the Oil Creek sandstone and varies between 0.4 and 13.0 wt. %.

The material from the Sulphur deposit was mixed with that obtained from Dougherty, and the resulting material, when used for paving purposes, apparently possessed superior qualities.

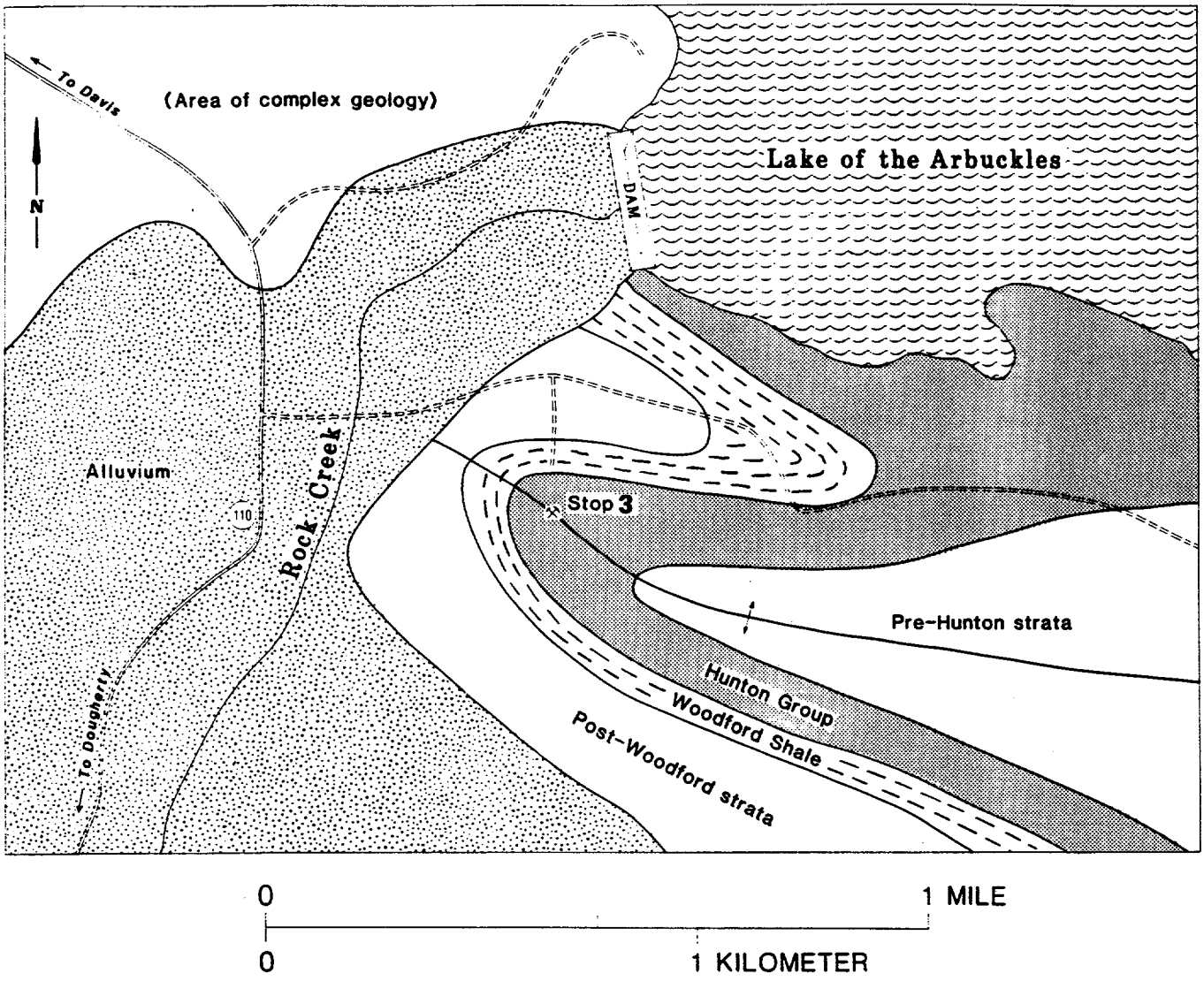

Figure **5** . Generalized geologic map of Stop **3** area, showing quarries along axis of northwest-plunging anticline. Adapted after Johnson and others (1984).

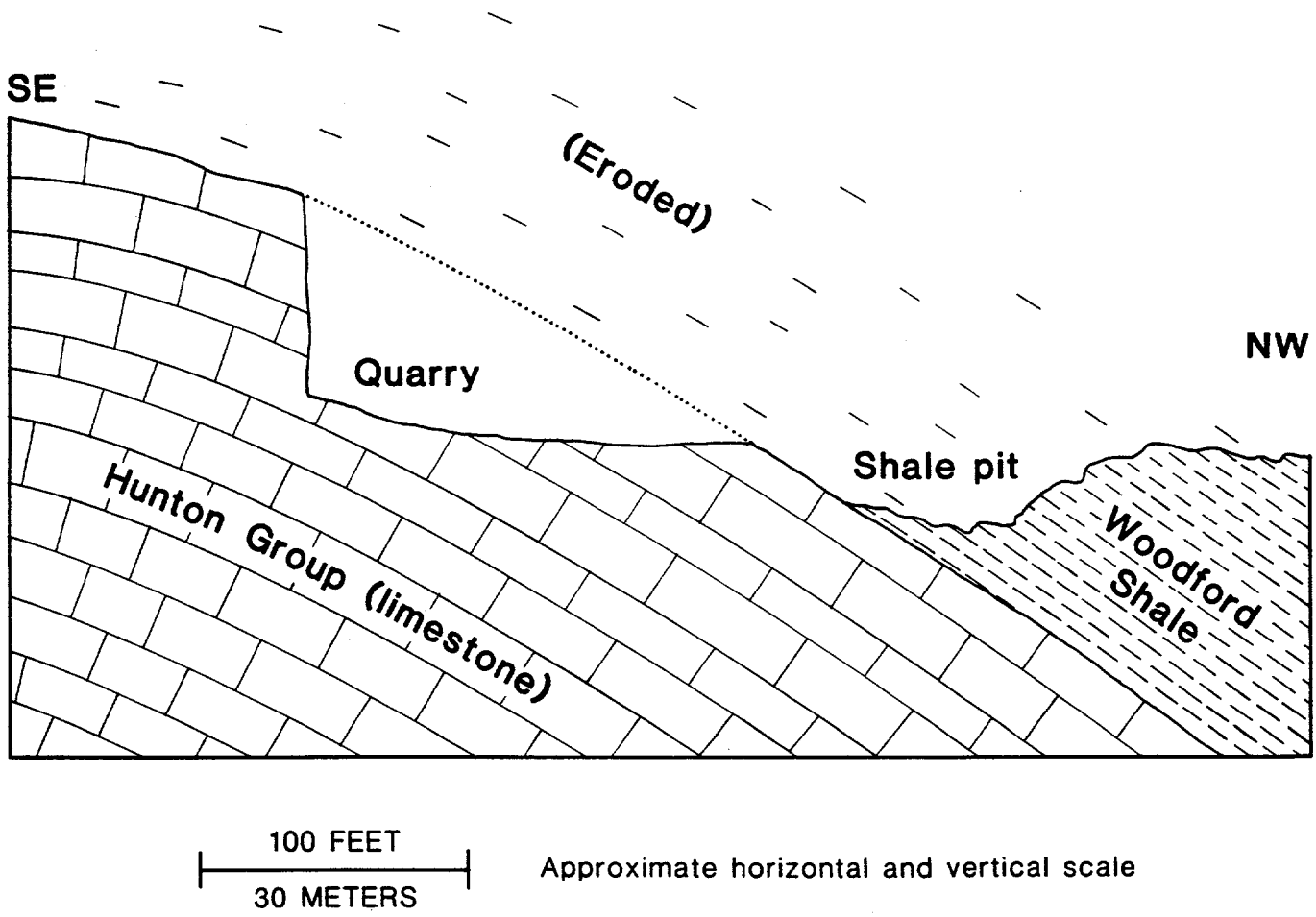

Figure **6**. Generalized cross section showing relationship of Hunton Group and Woodford Shale along axis of plunging anticline at Stop **3**. View looking toward southwest.
Source: Johnson and others (1984).

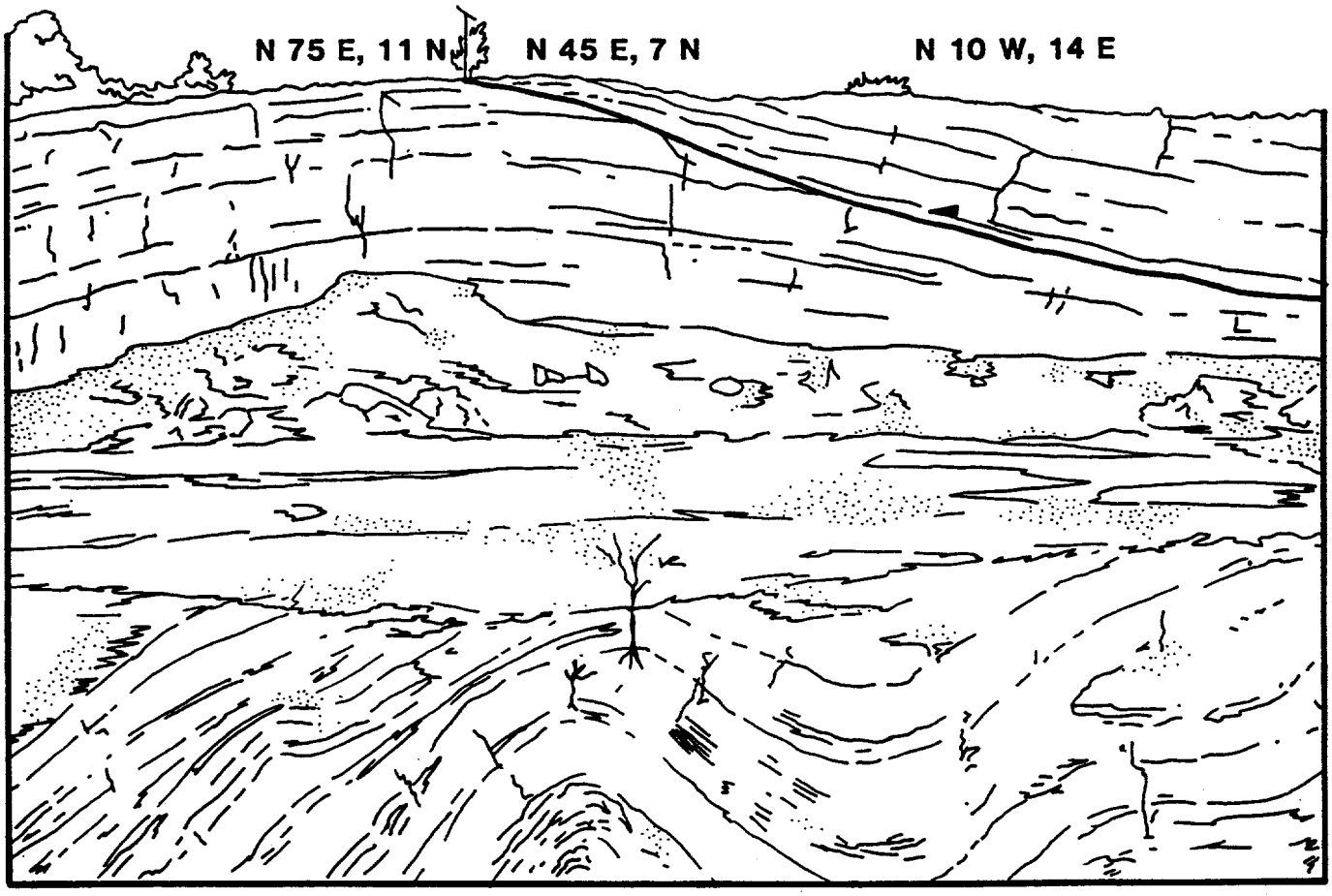

Fig. 7. Sketch of Hunton Quarry showing the low-angle thrust fault which is related to bedding plane slippage.
Source: Brown and others (1985).

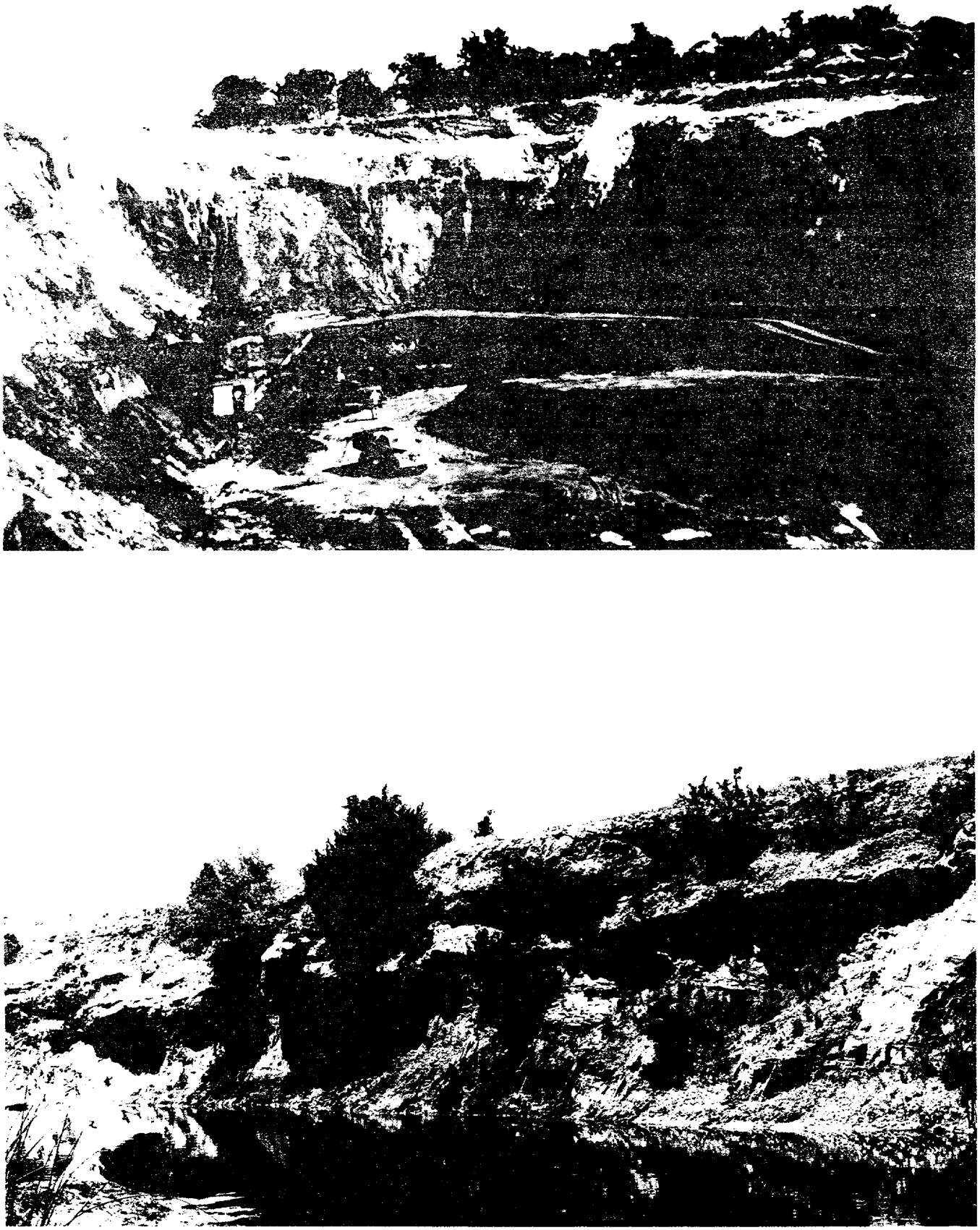

Figure 8. Two photographs of tar-sands quarry south of Sulphur. Above is view of open-pit mine that reached a depth of about 90 feet (27 m) before being abandoned in the 1950's. Below is a modern view of abandoned tar-sand quarry.
Source: Johnson and others (1984).

Figure 9 shows the geology of the Sulphur tar-sand area. Rock units that crop out in the Sulphur area include all formations of the Simpson Group, Viola Formation, Hunton Group, Woodford Formation, and Caney Formation (Williams, 1986). Bitumen stains are found in most of the rock units in the Sulphur area, with the most significant accumulation being in the Ordovician Oil Creek Formation of the Simpson Group. The Oil Creek is composed of two members: the upper Oil Creek limestone unit, a sequence of thinly interbedded limestones and shales, has a maximum thickness of 350 ft (105 m); the underlying Oil Creek sandstone member is a thick, massive, fine-grained sandstone. It is extremely well sorted and poorly cemented, which makes it an excellent reservoir rock. Layers of fine-grained dolomite or sandy dolomite are found within the unit, as well as locally hardened seams in which silica has been precipitated around the sand grains. The thickness of the Oil Creek sandstone ranges from 130 to 400 ft (39 to 122 m).

The structure of the Sulphur area is characterized by a northeast-southwest trending anticline cut by numerous faults. Gorman and others (1944) interpreted the faulting in the area as horst and graben-type block faulting. Williams (1986) reinterpreted the structure of the Sulphur area as being characterized by numerous thrust faults with associated high-angle reverse faulting. Figure 9 illustrates the structure of the Sulphur area in cross section. Williams' conclusions on the origin of faulting in the Sulphur area fit a model for right-handed wrench faulting preceded by left-handed wrenching. This corresponds with the currently popular theory of wrench tectonics as a mechanism for explaining structural features in southern Oklahoma.

According to Williams, it appears that hydrocarbons were first emplaced into the anticlinal structure. Subsequent faulting brought the hydrocarbon-saturated rocks into a position that left them susceptible to degradation of the hydrocarbons by processes of bacterial action, water washing, and inorganic oxidation. A second sequence of migration along faults and fractures may explain bitumen occurrences in overlying units such as the Vanoss conglomerate and the Viola limestone. In fact, pebbles of bitumen-saturated Oil Creek sandstone are found in the Vanoss conglomerate along with bitumen saturation in the sandy matrix of the conglomerate. This clearly suggests two periods of migration.

Bitumen saturation in the Oil Creek sandstone averages about 8 wt. %. API gravity of the bitumen has an average value of 4.22°. Based on current data, it is estimated that the Sulphur deposit contains about 33.8 million barrels of in-place heavy oil, with an additional 12.6 million barrels considered as probable reserves (Harrison and Burchfield, 1983).

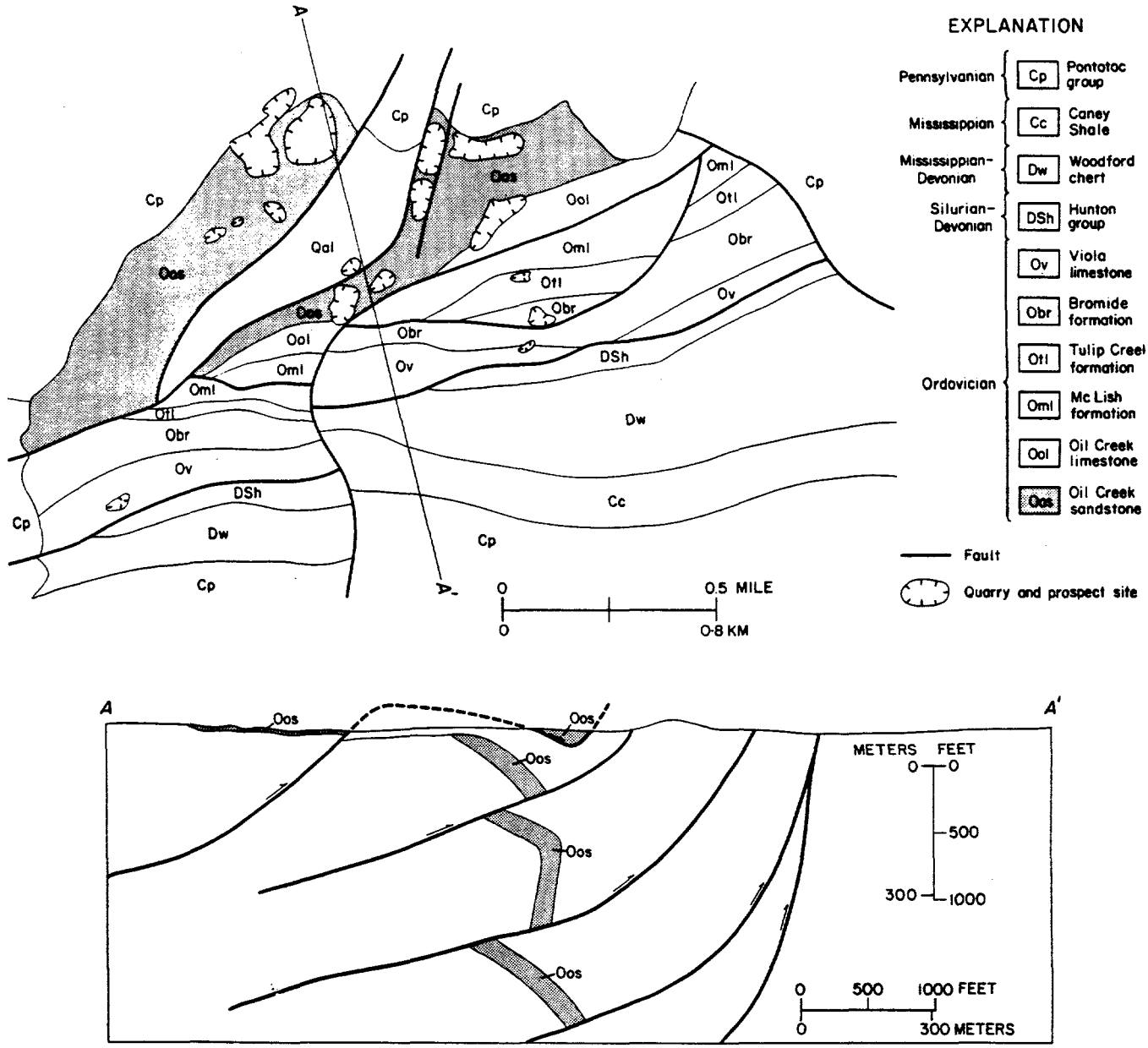

Figure 9. Geologic map (above) and interpretive cross section (below) of Sulphur asphalt area (Stop 4). Modified from Gorman and others (1944) and Williams (1983).
Source: Johnson and others (1984).

PALEOMAGNETIC DATING OF BASINAL FLUID MIGRATION, BASE-METAL MINERALIZATION, AND HYDROCARBON MATURATION IN THE ARBUCKLE MOUNTAINS, OKLAHOMA

D. S. Bagley, D. London, D. Fruit,
K. D. Cates, and R. D. Elmore
University of Oklahoma

ABSTRACT.—Paleomagnetic and rock magnetic results from the Ordovician Viola limestone in south-central Oklahoma indicate the presence of two chemical remanent magnetizations (CRMs). One is a CRM that is pervasive in the unfractured, non-mineralized Viola and resides in magnetite. An incremental fold test shows that this CRM was acquired during Pennsylvanian folding. Previous work has shown that the Viola was nonporous at the time of folding which probably excludes the possibility of remagnetization by externally derived fluids. A thermoviscous origin of this remagnetization can probably also be ruled out due to low maximum-burial temperatures. Because of this, an in situ chemical process of remagnetization, such as the maturation of hydrocarbons, is invoked to explain the pervasive synfolding magnetization.

A Permian CRM residing in hematite occurs in alteration halos around mineralized fractures. Geochemical studies indicate that the fluids that caused the mineralization and alteration were primarily basinal in origin, although multiple types of fluids were involved. The migration of basinal fluids through the fractures caused the remagnetization residing in hematite.

INTRODUCTION

The purpose of this paper is to describe paleomagnetic, petrographic, and geochemical results from the Viola limestone in the northern Arbuckle Mountains. The results have implications for understanding the timing and origin of base-metal precipitation in the northern Arbuckle Mountains (i.e., the Davis zinc field; Fay, 1981). In addition, the paleomagnetic results may have implications for determining the time of hydrocarbon maturation in the Viola.

GEOLOGIC SETTING

The study area is located within the Sooner rock and sand (SRS) quarry, secs. 11 and 14, T. 1 S., R. 1 E., Murray County, Oklahoma (Fig. 1). The quarry is in the Late Ordovician Viola limestone and is located ~3 km northeast of the Davis zinc field (Fay, 1981).

The Viola limestone is a widespread carbonate sequence as much as 300 m thick in the Arbuckle Mountains. At the base of the Viola are laminites that grade upward to coarse grainstones at the top of the unit. The Viola shallows upward and records deposition on a deep to shallow carbonate ramp (Ham, 1973; Galvin, 1983). The exposed limestone in the study area is interpreted to be lower to middle Viola. The limestones sampled are predominantly gray in color and consist primarily of fos-

siliferous mudstones, wackestones and some packstones that contain chert nodules. Primary porosities in these lithologies, particularly the mudstones and wackestones, are low. The limestones are tight, and other workers have suggested that any original porosity was occluded by an early phase of meteoric cementation (e.g., Grammer, 1985). The Viola does produce oil in some areas, but the porosity is a result of fracturing caused by deformation (Allen, 1983).

The Viola, which is found within the southern Oklahoma aulacogen (e.g., Wickham, 1978), was deposited during the subsidence stage that followed the rifting stage of the aulacogen. The aulacogen was reactivated during the Late Paleozoic, and during the deformation stage, the rocks in the aulacogen were intensely folded and faulted.

Within the SRS quarry is an anticline/syncline couplet (Fig. 2). The axes of the folds trend NNW–SSE and both plunge gently (5–6°) to the south. The limbs of the folds can be traced continuously in the quarry. Located on the eastern portion of the study area (east limb of easternmost anticline) (Fig. 3) is a fractured zone. The fractures in this zone have two general orientations. One set strikes approximately N. 25° W. and dips 50° to the southwest. This fracture set is apparently axial planar to the trend of the folds seen in the quarry. The second set of fractures strikes between N. 55° E. and N. 60° E., approximately normal to the axis of the folds and therefore likely to be extension fractures (Wiltse, 1978). In one area the rocks are highly fractured and brecciated. This zone, which contains an abundance of small scale slickensides, is interpreted to be the surface expression of a fault which trends NNW–SSE and dips to the west.

Some of the fractures are mineralized with calcite. The calcite mineralization provides evidence of fluid migration through the fault zone. Also associated with the calcites in the fractures are Mississippi Valley-type base metal oxides and sulfides including sphalerite, pyrite, marcasite, and goethite. In addition to the calcite mineralization, the fractures in this zone often exhibit a pipe-like appearance (Fig. 4), and some of the fractures are conduits for tar seeps. This zone will be referred to as the "mineralized zone" (Fig. 3).

The Viola in direct contact with the mineralized fractures and in the brecciated zone is commonly altered from the normal gray Viola to a yellow to reddish color. The calcite in the fractures also extends into the rock along what are apparently small fractures. In addition, a red to yellow, fine-grained carbonate-clay material can occur at the contact between the host limestone and the calcite in the fractures. This material also partially to completely fills some vugs and small fractures in the limestones. This material is clearly secondary and is probably related to the mineralizing event.

The western limb of the anticline and the adjacent syncline exhibit significantly less fracturing, and calcite mineralization and tar seeps are absent (Fig. 5). This zone will be referred to as the "non-mineralized zone" (Fig. 3).

Within and around the limestone quarry are a number of oil wells that comprise the Southwest Davis oil field. Oil production in the field comes primarily from the Oil Creek sand-

stones at depths of 1,000–1,600 m. Previous work has shown that the hydrocarbons in the field were trapped as a result of a thrust-fault system and its associated en echelon faults (Wiltse, 1978). Evidence for thrust faulting is shown by demonstrating that the Oil Creek is repeated a number of times in different wells within the field.

MINERALOGY OF CALCITE-FILLED VEINS

The mineralogy of the calcite-vein filling is surprisingly complex, but can be subdivided into two stages of growth: early, basal scalenohedra (S) that project in the fractures and cavities, and later, crystallographically complex rhombohedral overgrowths (R) on the scalenohedra. The calcites also occur in two distinct environments: those that are covered with natural asphalt (designated YA), and those that lack any evidence of associated hydrocarbons (NA). Thus, there are four parageneses of calcite: SYA, SNA, RYA, RNA, each with the following distinctive characteristics or associated mineral assemblages.

Fluorescence.—In short-wave ultraviolet (UV), SNA show white fluorescence and strong phosphorescence at their bases, changing to orange fluorescence at the tips of crystals. RNA fluoresce red, especially within an inner-growth zone of included minerals and fluids. SYA rarely exhibit the same white fluorescence and phosphorescence at their bases, but generally SYA and all RYA are not fluorescent.

Morphology.—The most striking and significant difference in growth forms involve the rhombohedral overgrowths. RNA are flat-faced rhombohedra twinned on {0001}, with smooth, sometimes slightly etched surfaces. RYA are rounded untwinned rhombohedra, generally with very shiny surfaces marked by macroscopic, flat-faced circular growth steps.

Associated Minerals.—Neither SYA nor SNA contains included solids; however, marcasite + sphalerite are deposited along the surface contacts between SNA and RNA. Multiple growth zones of marcasite + goethite lie within RNA, but are absent in RYA. Where the tips of SYA project through RYA overgrowths, these SYA tips and adjacent RYA surfaces are covered with sphalerite + marcasite. Sphalerite + pyrite ± marcasite are also abundant as fine-grained druses covering the open undersurfaces of the YA vein calcites.

Fluid Inclusions.—Primary fluid inclusion populations in SYA and SNA are indistinguishable. Both are marked by aqueous saline Na–Ca–brines (designated DCB for divalent cation brine) entrapped at approximately 80–90°C. Primary spherical fluid inclusions associated with marcasite + goethite bands in RNA are mostly saline Na-brines (designated MCB, for monovalent cation brine) entrapped at approximately 50–60°C (Fig. 6). These occur with minor numbers of closely associated inclusions containing Na–Ca–brines similar to those in SNA. No fluid inclusions have been found in

RYA. All calcites contain secondary fluid inclusions (non-saline, low temperature) that apparently represent entrapment of near-surface meteoric water (designated MW).

The inferred chemistry and depositional sequence based on fluid inclusion and petrographic/microprobe studies are summarized below.

1) Basal scalenohedra (S) were deposited from normal saline basinal brines (DCB) at temperatures of approximately 80–90°C.

2) Rhombohedral overgrowths (RNA) were deposited primarily in the presence of a different, Na-dominated brine (MCB) at temperatures of 50–60°C. In the NA associations, the change from DCB to MCB (perhaps cooler, lower pH, and/or more oxidizing) may have caused the precipitation of marcasite + sphalerite at SNA–RNA contacts. The presence of DCB and MCB inclusions in the marcasite + goethite growth zones of RNA suggest (1) continued fluid mixing of DCB and MCB, with increasing dominance of MCB; and (2) increasing oxidation state and decreasing pH of fluids associated with RNA (chemical properties that may have been intrinsic to MCB, and representative of increasing MCB/DCB volumetric ratios).

3) Unfortunately, there are no complementary inclusions in RYA; however, the absence of Fe-oxides in YA associations suggest that the fluids responsible for deposition of SYA and RYA remained more reduced and perhaps more sulfur-rich than those in NA associations until sphalerite + marcasite were deposited on the tips and outer surfaces of YA-associated calcites. In this connection, the circular growth steps on RYA surfaces are interpreted as the result of calcite deposition in a two-phase fluid suspension, inferred to be largely immiscible aqueous brine (DCB?) + petroleum. The presence of petroleum would maintain higher sulfide activities and lower oxidation states in associated brines, leading to precipitation of abundant and very late-stage sphalerite. These inferences and observations lead to some important and unresolved questions regarding the age of the asphalts in seeps, the time of the culmination of calcite (RYA) precipitation, and the possibility that modern asphalts in YA veins represent recent seeps, but that YA fractures have been conduits for petroleum over a long period of geologic time (see paleomagnetic results). In any case, the fluids migrating through these fractures (NA versus YA) remained clearly distinct, at least through the later stages of calcite deposition (R).

4) Low temperatures of formation, comparatively low Fe contents of sphalerite, and the total absence of galena and Cu-sulfides suggest that the SRS quarry lies near a distal (cooler, shallower?) edge of the Davis zinc field. At this level of burial, apparently four distinct fluids (DCB, MCB, MW, and petroleum) were introduced through fractures and mixed to various degrees. These complex fluid relations would have provided variable Eh, pH, sulfide activities, salinities, and temperatures leading to gross oxide/sulfide zoning patterns, and through mixing promoting oxide/sulfide precipitation.

PALEOMAGNETISM

Mineralized Zone

Thermal demagnetization of specimens taken from within the calcite-filled fractures indicates the presence of two magnetic minerals. One phase shows significant decay by 100°C, while the other decays to 680°C (Fig. 7). Because goethite has a Curie temperature of 100°C and hematite has a Curie temperature of 680°C, these two minerals are the likely magnetic phases present in the calcites. Random directions were recorded for samples from the goethite and hematite in coarse vein-filling calcites.

Rock magnetic experiments conducted on the limestones in direct contact with the fractures indicate the predominance of a high coercivity mineral (Fig. 8A) with maximum unblocking temperatures of 680°C (Fig. 8B). In these specimens, the magnetization resides predominantly in hematite. With increased distance from the fractures, the amount of alternating field (AF) decay increases significantly, suggesting the emergence of a low coercivity phase. The low coercivity mineral is probably magnetite, while the high coercivity mineral that decays to 680°C is hematite. All lines of evidence indicate that as distance from the fractures increases, the relative ratio of the high coercivity hematite to the low coercivity magnetite decreases. It is apparent, then, that there is an alteration halo surrounding fractures with a magnetization residing in hematite (Fig. 9). It is believed that the fluids moving through the fractures and causing the mineralization were also responsible for the remagnetization and change in magnetic mineralogy.

The mean direction for the limestones in direct contact with the fractures was south–southeasterly and shallow (Fig. 10). The pole position for specimens in direct contact with the fractures is 109° E. longitude, 51° N. latitude, which corresponds to a Late Permian pole (Fig. 11) on the North American Apparent Polar Wander Path of Irving and Irving (1982). A similar pole position was also found for the rocks in the highly fractured and brecciated zone (Fig. 11).

Non-Mineralized Zone

The results of rock magnetic experiments indicate that the samples from the non-mineralized zone are dominated by a single, low coercivity magnetic phase (Fig. 8A) that decays completely by 580°C (Fig. 8B). Magnetite is a low coercivity mineral with a Curie temperature of 580°C and carries the magnetization in the non-mineralized zone. The directions for this component are southeasterly and shallow, and the directions from the limbs of the fold cross when the rocks are corrected for the tilt (Fig. 12). The results of an incremental fold test indicate that the magnetization was acquired during Pennsylvanian folding (Fig. 13). A statistically significant grouping of site means occurs at 70% unfolding (Fig. 13). The resultant pole position (126.5° E. longitude and 34.8° N. latitude) plots near the Early Carboniferous segment of Irving and Irving's (1982) Apparent Polar Wander Path (Fig. 11).

The origin of the magnetization in the non-mineralized zone is somewhat problematic. Thermoviscous processes can be ruled out as the Viola experienced only relatively low burial temperatures (e.g., Metcalf, 1985). Thus a chemical origin of remagnetization is invoked. It is also likely that the process by which the magnetization was acquired was an in situ process, as the limestone is extremely tight and any original porosity was probably eliminated by an early phase of meteoric cementation (Grammer, 1985).

In a previous study of the Viola on the Arbuckle Anticline (south of the SRS study area) Peck and Elmore (1984) reported that the unit contains a magnetization, interpreted to be a chemical remnant magnetization (CRM), residing in magnetite. The directions from each flank crossed during unfolding, although the corrected directions from the south flank (141/3) are close to the uncorrected directions from the north flank (146/3). The directions from the south flank of the Arbuckle Anticline are important because they are similar (141/16, 70% tilt correction) to the direction at the SRS locality. The SRS locality is between the Washita Valley and Reagan faults, which defines a structurally complex area deformed by wrench faulting (Wickham, 1978) and perhaps gravity sliding (Phillips, 1983). These processes could have rotated structural blocks around a vertical axis. The similarity in the directions between the SRS locality, where there is the possibility of rotation, and the south flank of the Arbuckle Anticline, where rotation is unlikely, suggests that the SRS locality has not been rotated. The north flank of the Arbuckle Anticline is in the area that could have been rotated; the strike of the beds (N. 60° W.) is significantly different than for the SRS locality (N. 25° W.). The directions from this locality could be rotated or, alternatively, they could indicate asymmetrical folding.

DISCUSSION

The Viola Formation in the Arbuckle Mountains contains a pervasive Pennsylvanian synfolding CRM in magnetite and locally a Permian CRM in hematite that is related to migration of basinal fluids. Based on comparisons with blocking temperature/relaxation time curves (e.g., Middleton and Schmidt, 1982), the magnetizations cannot be thermoviscous in origin due to the low burial temperatures.

The pervasive CRM in magnetite is similar to other synfolding magnetizations, some interpreted to be CRMs, reported from other carbonate units (e.g., McCabe and others, 1983). Lateral migration of orogenic fluids has been suggested as the agent of remagnetization for some of these units, although this interpretation probably cannot apply to the Viola. In the areas studied, except for the fractured zones, the Viola does not contain significant porosity and probably did not prior to folding (Grammer, 1985). Because the unit was probably tight at the time of folding, fluids could not have pervasively entered the rock. An in situ chemical mechanism, therefore, is needed to explain the remagnetization.

There are several diagenetic processes that occurred in the Viola and may be related to magnetite authigenesis. For example, the Viola contains organic matter in the study area and one possible in situ mechanism could be related to diagenesis of this organic matter. Total organic carbon (TOC) values range between 0.04 and 0.54% for the Viola in the study area. Based on preliminary Rock-Eval pyrolysis, S_1/S_1+S_2 ratios range from 0.06 to 0.21 and T_{max} ranges from 434 to 442°C. These results suggest that some of the rocks are immature, but others have just entered the oil window (Tissot and Welte, 1984). The results are also consistent with the interpretation that the hydrocarbons were generated in situ. The chemical conditions created by the maturation of the hydrocarbons may have caused precipitation of authigenic magnetite and acquisition of the synfolding CRM. This interpretation is consistent with the geologic history; maturation of hydrocarbons probably occurred during maximum burial and heating, and this may have coincided with the time of folding. Another mechanism that may be related to magnetite authigenesis is the transformation of smectite to illite which releases iron (Boles and Franks, 1979). The Viola contains some illite, and relatively thick volcanic ash deposits are found in the lateral equivalent of the Viola to the southeast (Sediqi, 1985).

Both maturation of hydrocarbons and the smectite–illite reaction can be caused by burial temperatures (100°C) that are not high enough to cause a thermoviscous remagnetization. These, or other, in situ chemical processes mediated by relatively low burial temperatures could explain the pervasive CRM in the Viola as well as other pervasive magnetizations in carbonates. These hypotheses for in situ chemical remagnetization, however, are untested.

The Permian CRM residing in hematite is primarily related to basinal fluids that migrated along the fracture and fault zones. We suggest that mixing of different fluids (basinal, meteoric) and interactions between these fluids and the organic-rich Viola caused precipitation of the iron oxides and remagnetization around the fractures.

ACKNOWLEDGMENTS

The authors thank Karen Cochran and Mike Engel for input on the organic geochemistry of the Viola. Support was provided by grants from the National Science Foundation (EAR 8917181) and the Oklahoma Mining and Minerals Resources Research Institute to Elmore and London.

REFERENCES

Allen, G. D., 1983, Origin and genesis of fracture porosity in Viola limestone (Ordovician) [abstract]: American Association of Petroleum Geologists Bulletin, v. 67, p. 411.

Boles, J. R.; and Franks, S. G., 1979, Clay diagenesis in Wilcox sandstones of southwest Texas: implications of smectite diagenesis on sandstone cementation: Journal of Sedimentary Petrology, v. 49, p. 55–70.

Fay, R. O., 1981, Geologic map of southwest Davis zinc field, Arbuckle Mountains, Oklahoma: Oklahoma Geological Survey Map GM-20, 1 sheet, scale 1:7,920, 16-page text.

Fisher, R. A., 1953, Dispersion on a sphere: Proceedings of the Royal Society of London, Series A, v. 217, p. 295–305.

Galvin, P. K., 1983, Deep-to-shallow carbonate ramp transition in Viola limestone (Ordovician), southwest Arbuckle Mountains, Oklahoma [abstract]: American Association of Petroleum Geologists Bulletin, v. 67, p. 466.

Ham, W. E., 1973, Regional geology of the Arbuckle Mountains, Oklahoma: Oklahoma Geological Survey Special Publication 73-3, 61 p.

Irving, E.; and Irving, G. A., 1982, Apparent polar wander paths Carboniferous through Cenozoic and the assembly of Gondwana: Geophysical Surveys, v. 5, p. 141–188.

McCabe, C.; Van der Voo, R.; Peacor, D. R.; Scotese, C. R.; and Freeman, R., 1983, Diagenetic magnetite carries ancient yet secondary remanence in some Paleozoic sedimentary carbonates: Geology, v. 11, p. 221–223.

Metcalf, W. J., 1985, Investigation of paleotemperatures in the vicinity of the Washita Valley fault, southern Oklahoma: University of Oklahoma unpublished M.S. thesis, 94 p.

Middleton, M. F.; and Schmidt, P. W., 1982, Paleothermometry of the Sidney basin: Journal of Geophysical Research, v. 87, p. 5351–5359.

Peck, C. J.; and Elmore, R. D., 1984, Paleomagnetism of the Ordovician Viola limestone, south-central Oklahoma [abstract]: EOS, v. 65, p. 197–198.

Phillips, E. H., 1983, Gravity slide thrusting and folded faults in western Arbuckle Mountains and vicinity, southern Oklahoma: American Association of Petroleum Geologists Bulletin, v. 67, p. 1363–1390.

Sediqi, A. S., 1985, A sedimentologic and geochemical study of the Bigfork chert in the Ouachita Mountains and the Viola limestone in the Arbuckle Mountains: University of Oklahoma unpublished Ph.D. dissertation, 155 p.

Tissot, B. P.; and Welte, D. H., 1984, Petroleum formation and occurrence [second edition]: Springer-Verlag, New York, 699 p.

Wickham, J. S., 1978, The southern Oklahoma aulacogen, *in* Wickham, J. S.; and Denison, R. E. (eds.), Structural style of the Arbuckle region: Geological Society of America, Guidebook for South-Central Section Annual Meeting, Field Trip 3, p. 9–41.

Wiltse, E. W., 1978, Surface and subsurface study of the southwest Davis oil field, sections 11 and 14, T. 1 S., R. 1 E., Murray County, Oklahoma: University of Oklahoma unpublished M.S. thesis, 72 p.

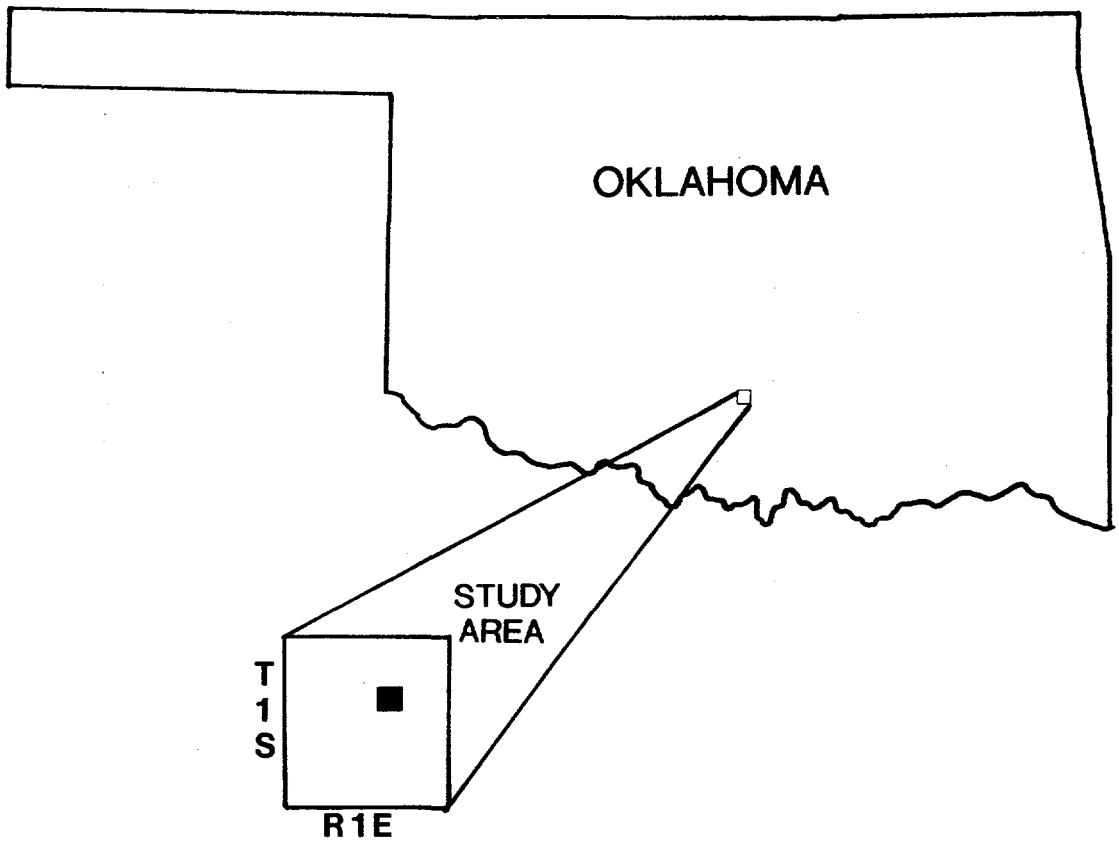

Figure 1. Map of Oklahoma showing study area located in Murray County, south-central Oklahoma.

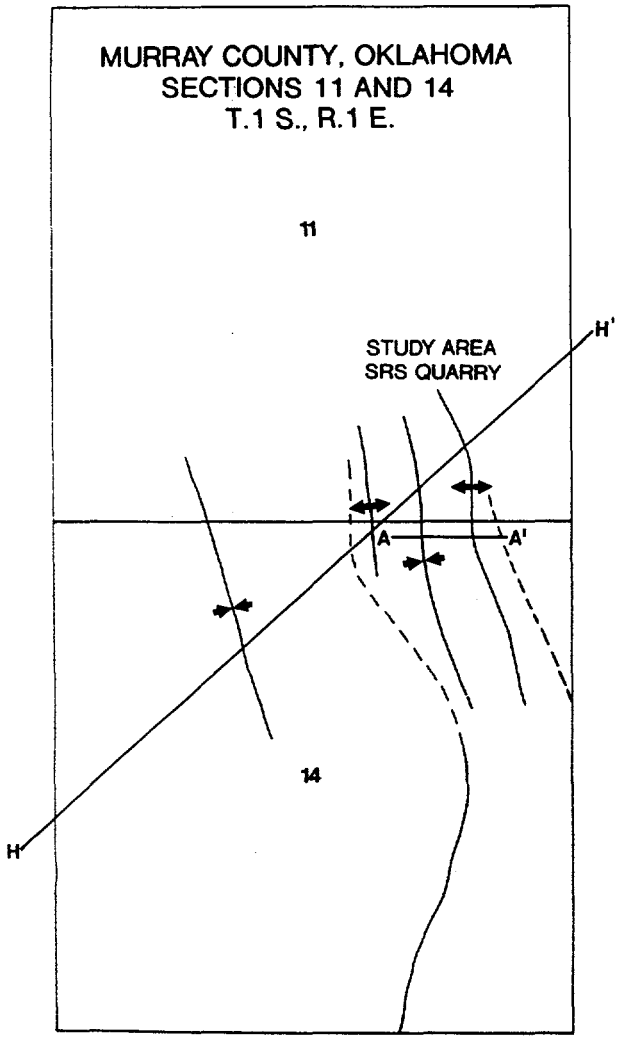

Figure 2. Figure showing structural features in the vicinity of the Sooner rock and sand quarry (after Wiltse, 1978).

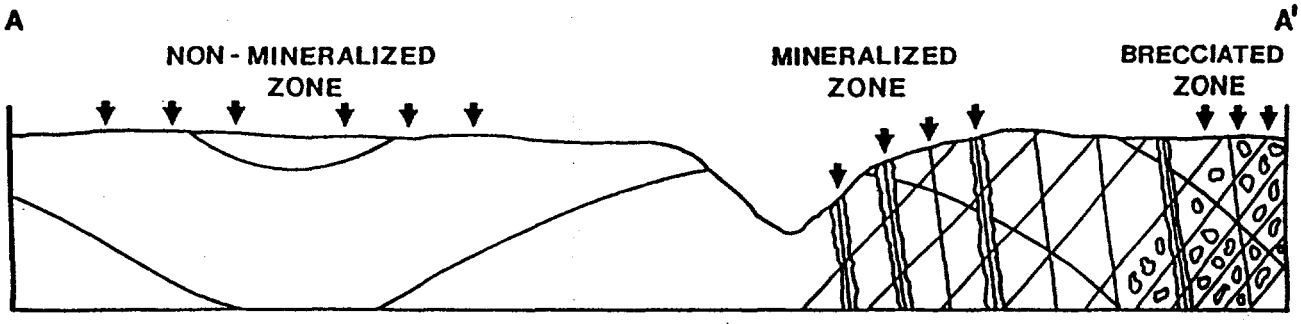

Figure 3. Sketched cross section A–A′ of the study area showing the zones sampled and the sample-site locations (arrows).

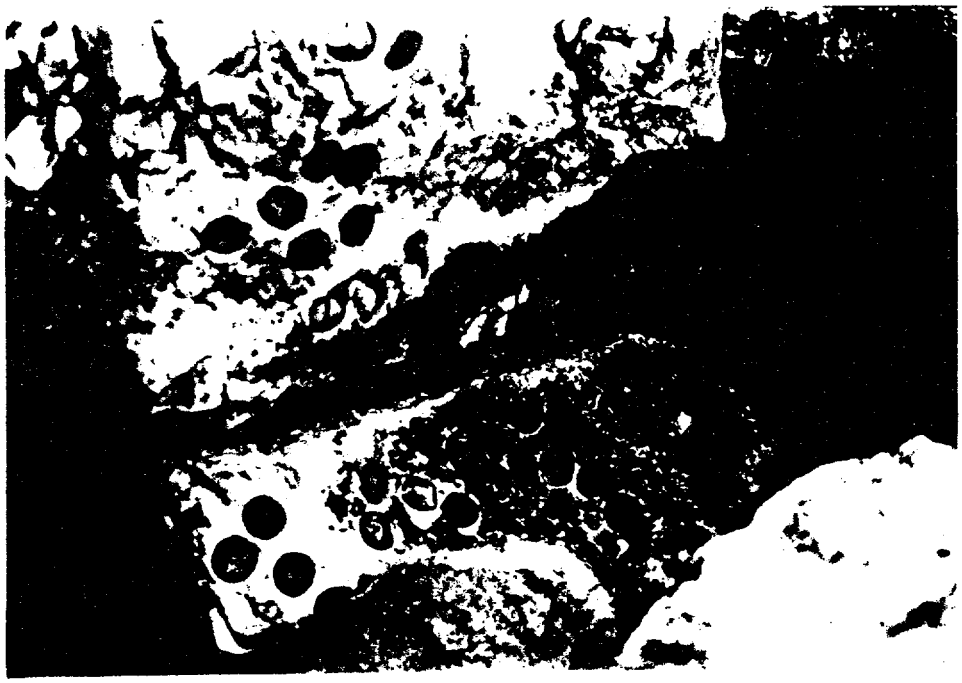

Figure 4. Field photograph from the mineralized zone. Note the hollow, pipe-like fracture that is lined with calcite.

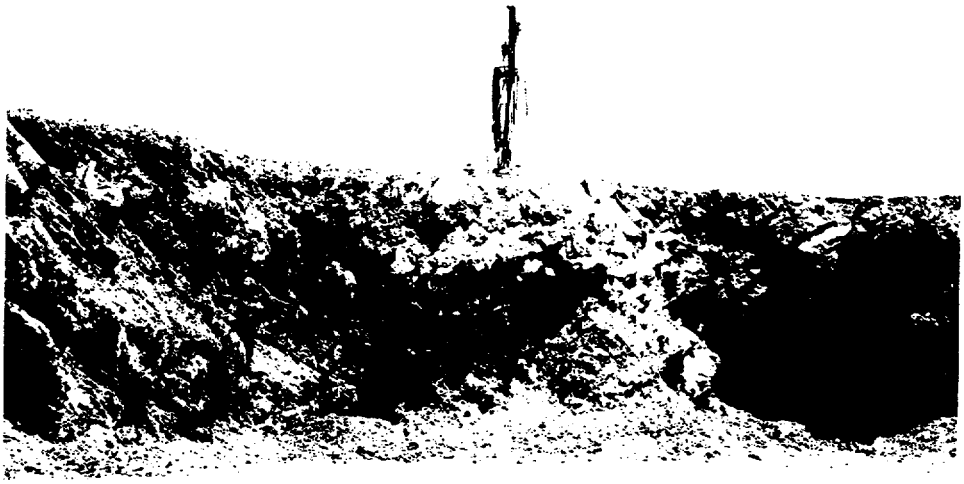

Figure 5. Field photograph of folded Viola limestone in the non-mineralized zone.

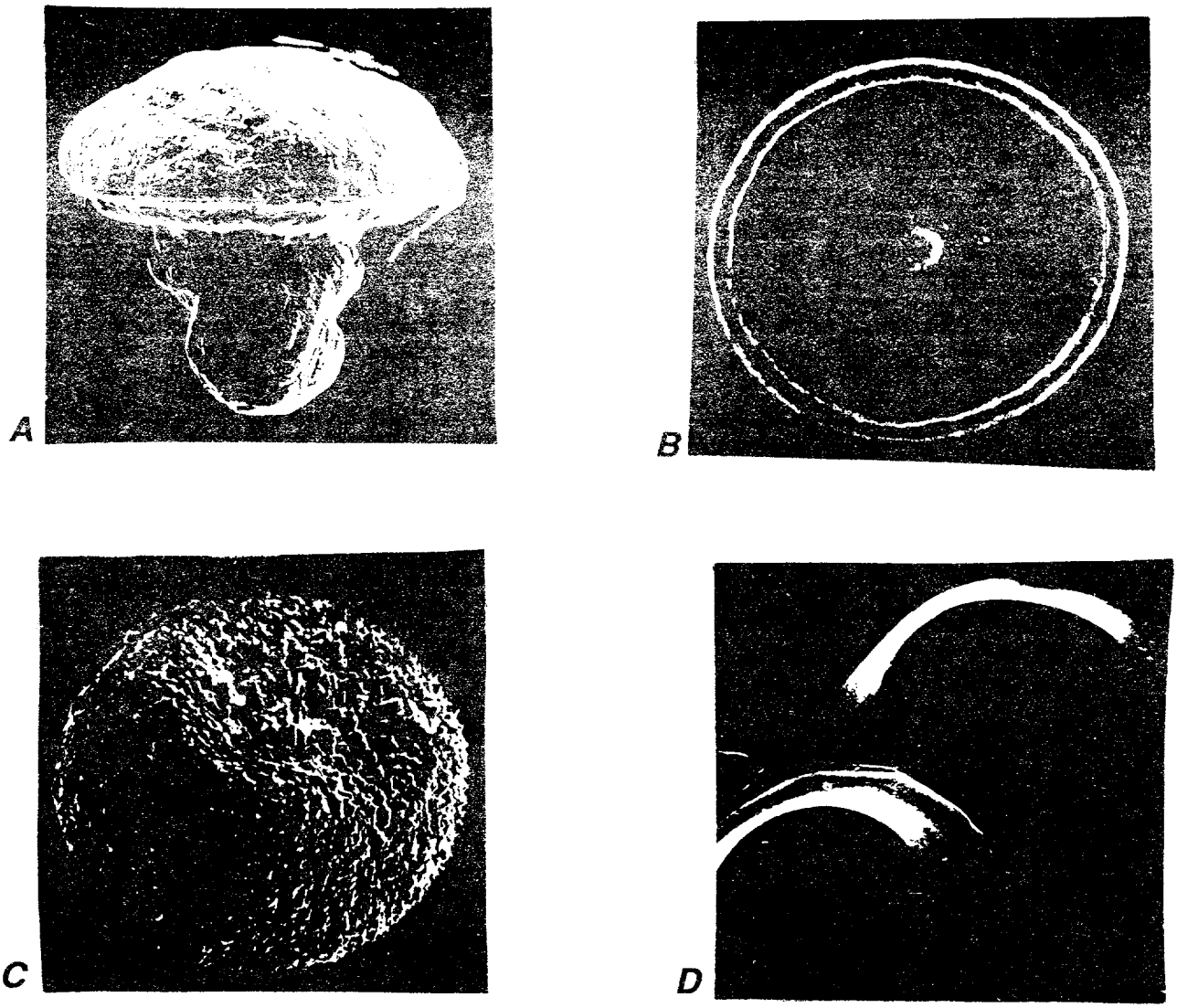

Figure 6. Electron photomicrographs of calcite and some commonly associated oxide and sulfide phases. *A*—Cross section of primary, mushroom-shaped goethite or hematite crystal aggregate, dissolved out of an inclusion-rich layer within RNA calcite. The stems of the mushrooms point to the interior of the calcite rhombs, the caps lie toward the exterior of calcite crystals. Such Fe-oxide inclusions were deposited on the growth surfaces of RNA calcites, and subsequently overgrown by calcite to form inclusions within rhombs (magnification 70×). *B*—View from the base of an Fe-oxide mushroom, showing the radial composite structure (mushroom gills) of very fine-grained Fe-oxide needles that constitute the cap of such aggregates (magnification 700×). *C*—A composite radial sphere of marcasite crystals, removed from the exterior tip of SYA calcites where these project through RYA overgrowths. More commonly, marcasite forms thin-bladed, single crystals or rosettes of intergrown-bladed crystals as inclusions within calcites (at SNA–RNA boundaries and within some RNA inclusion-rich growth zones; magnification 275×). *D*—Surface topography of RYA calcites, showing the flat-topped circular growth platforms that are found only on rhombic calcite overgrowths associated with asphalt seeps (magnification 100×). Common base-metal phases not shown in this figure are associated pyrite (modified octahedra that coat the altered limestone matrix in YA-calcite associations), and sphalerite (complex octahedral and tetrahedral composite crystals that are found mostly on the exterior tips of SYA where these project through RYA overgrowths).

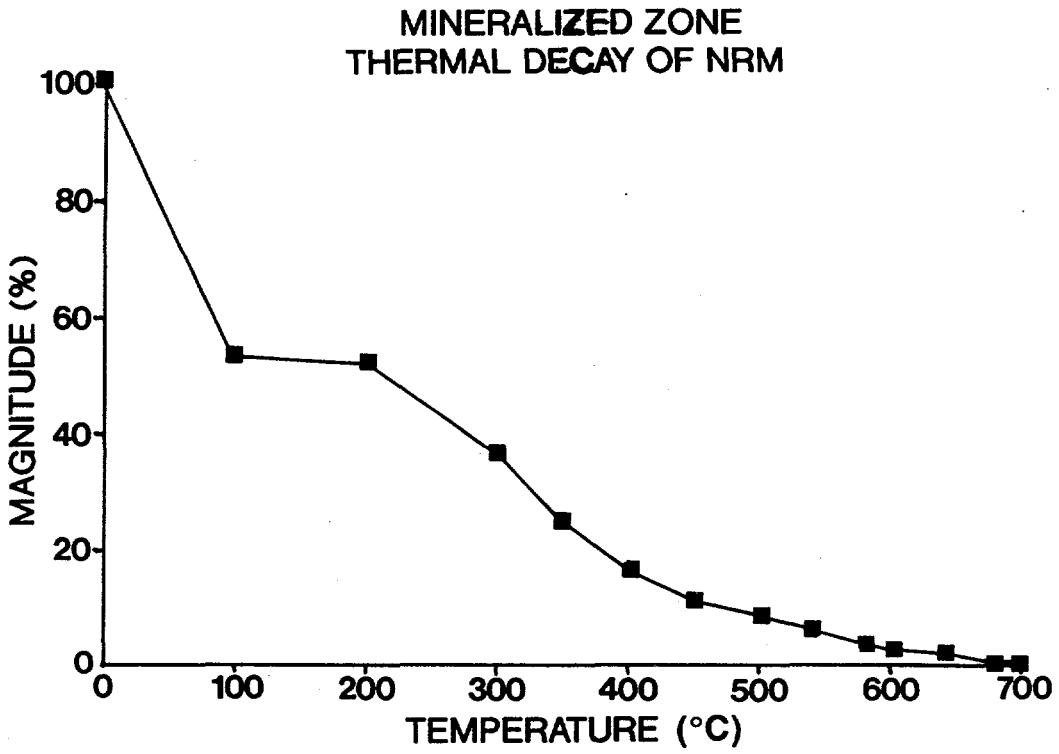

Figure 7. Representative thermal demagnetization curve for a specimen from the calcite in the veins.

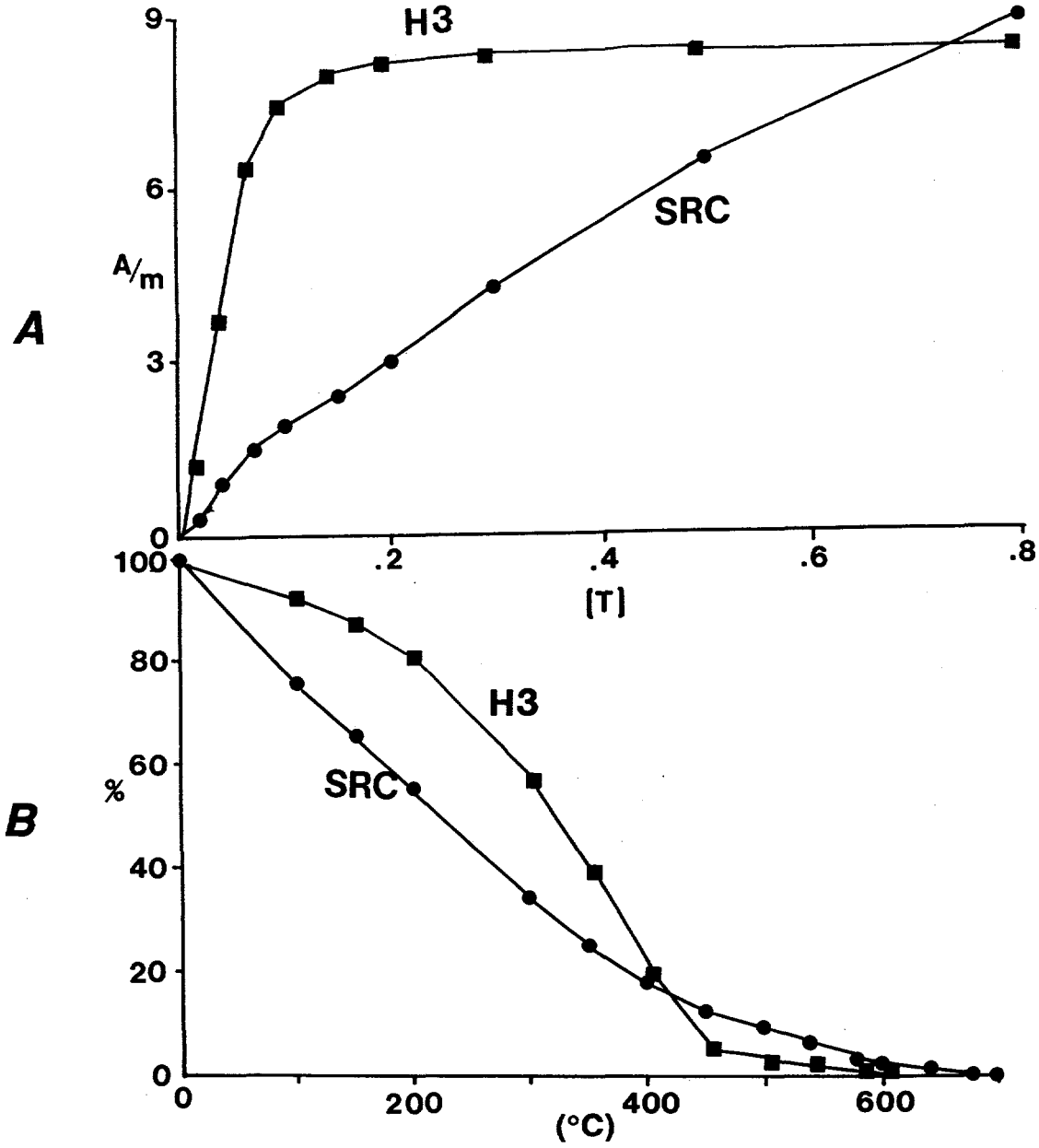

Figure 8. *A*—Representative IRM acquisition curves for limestone specimens in the mineralized (SRC) and non-mineralized (H3) zones. Curve SRC does not achieve saturation by 0.63 T. Note small cusp in curve at 0.1 T, which suggests the presence of a minor amount of a low coercivity phase. The rise in the curve above 0.2 T indicates the presence of a high coercivity phase. Curve H3 reaches saturation by 0.2 T, indicating the presence of a low coercivity mineral. *B*—Representative thermal decay of IRM curves for specimens in the mineralized and non-mineralized zones. Decay above 580°C in SRC suggests the presence of hematite. Note maximum unblocking temperatures of 580°C for curve H3, which suggests the magnetic phase is magnetite.

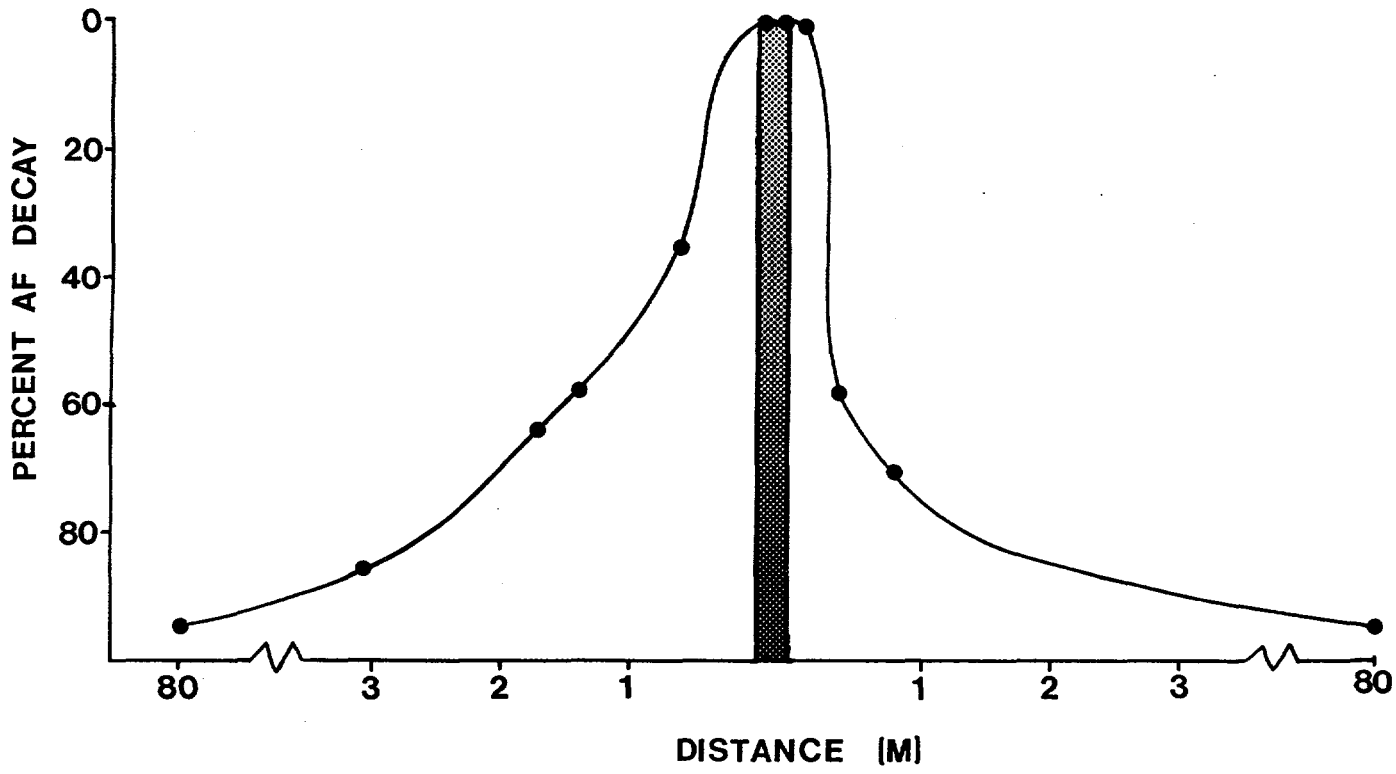

Figure 9. Summary diagram showing percent of AF decay of NRM as a function of distance from the calcite-filled fractures. Note that the highest coercivity (low AF decay) specimens are located within or very close to the fracture, but as distance increases a low coercivity (high AF decay) phase begins to emerge.

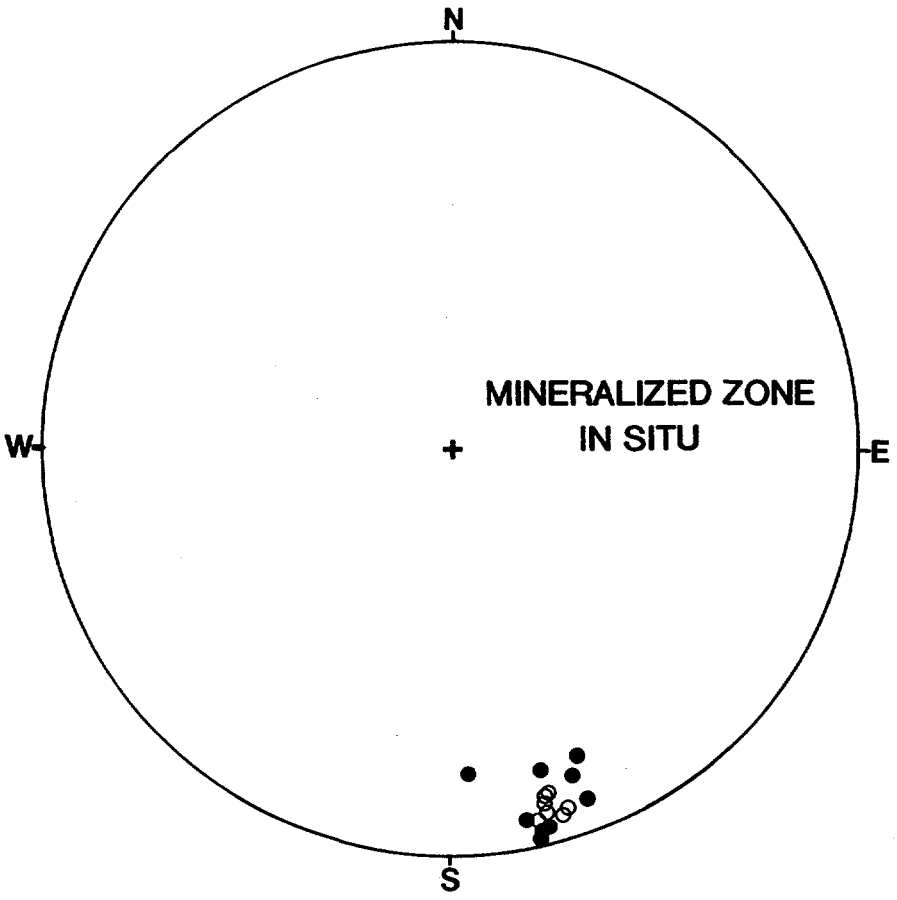

Figure 10. Schmidt equal-area projection for specimens in the mineralized zone in direct contact with a calcite-filled fracture. Direction (in situ) is south–southeast and shallow. Solid symbols represent projections in the lower hemisphere, open symbols represent projections in the upper hemisphere.

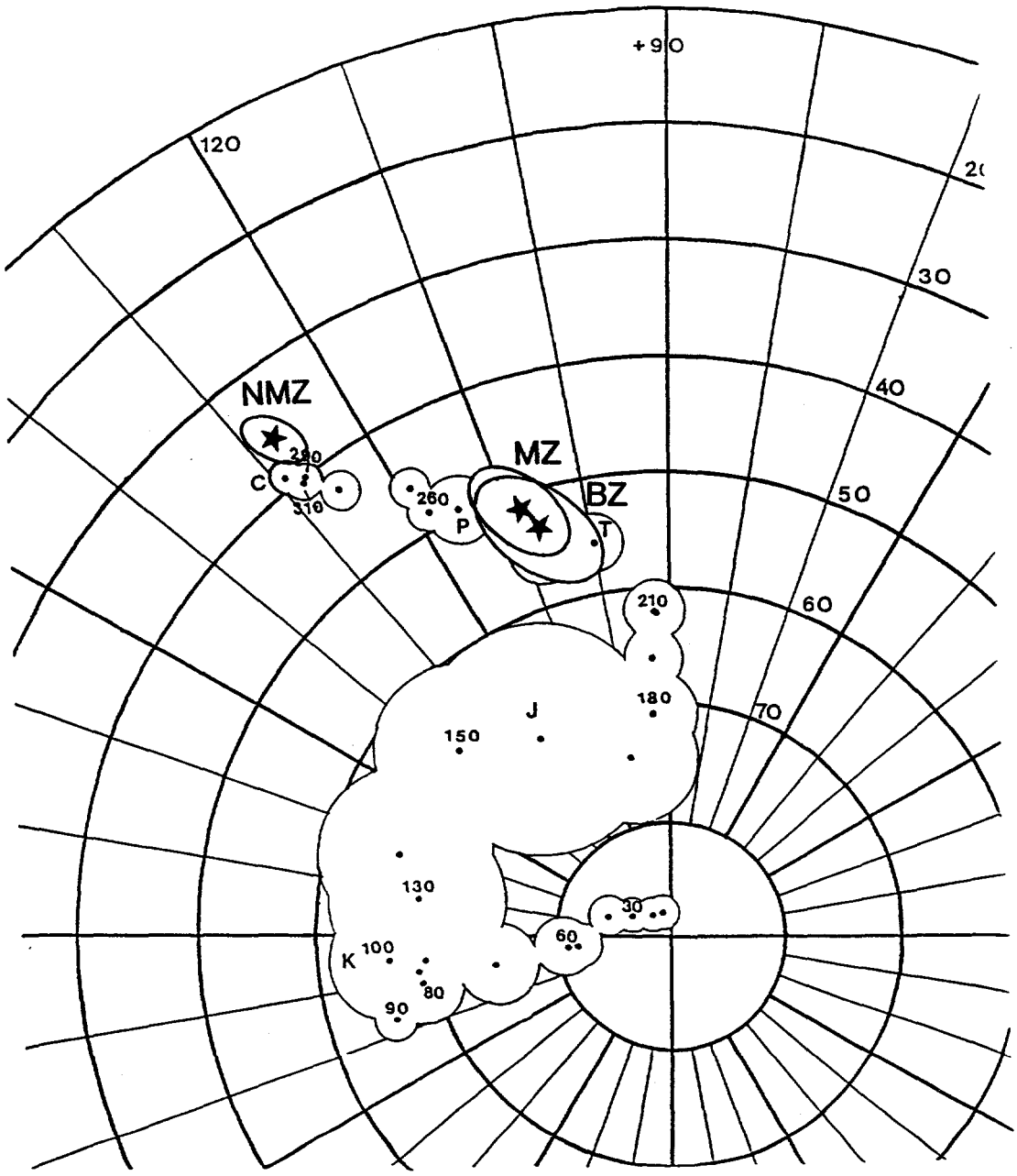

Figure 11. North American Apparent Polar Wander Path (Irving and Irving, 1982), with the paleo-poles calculated from the mean magnetic directions of the non-mineralized zone (NMZ), the mineralized zone (MZ), and the brecciated zone (BZ). The poles are plotted with their ellipses of confidence.

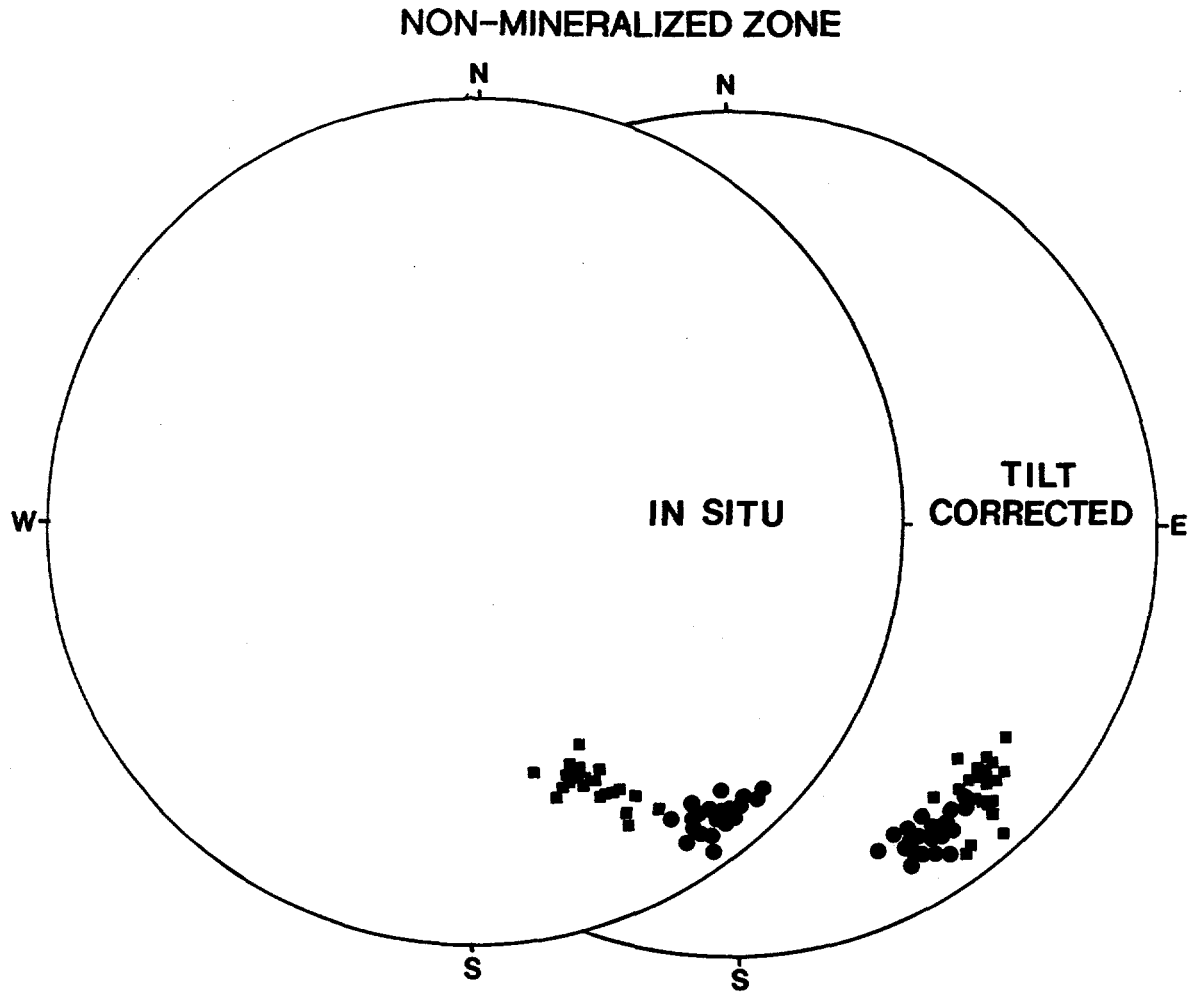

Figure 12. Schmidt equal-area projection of specimens from six sites in the non-mineralized zone, before and after tilt correction. Square symbols represent specimens from E-dipping limb, circles are from W-dipping limb (all specimens plot on lower hemisphere). Note that the directions cross during complete tilt correction, indicating a synfolding magnetization.

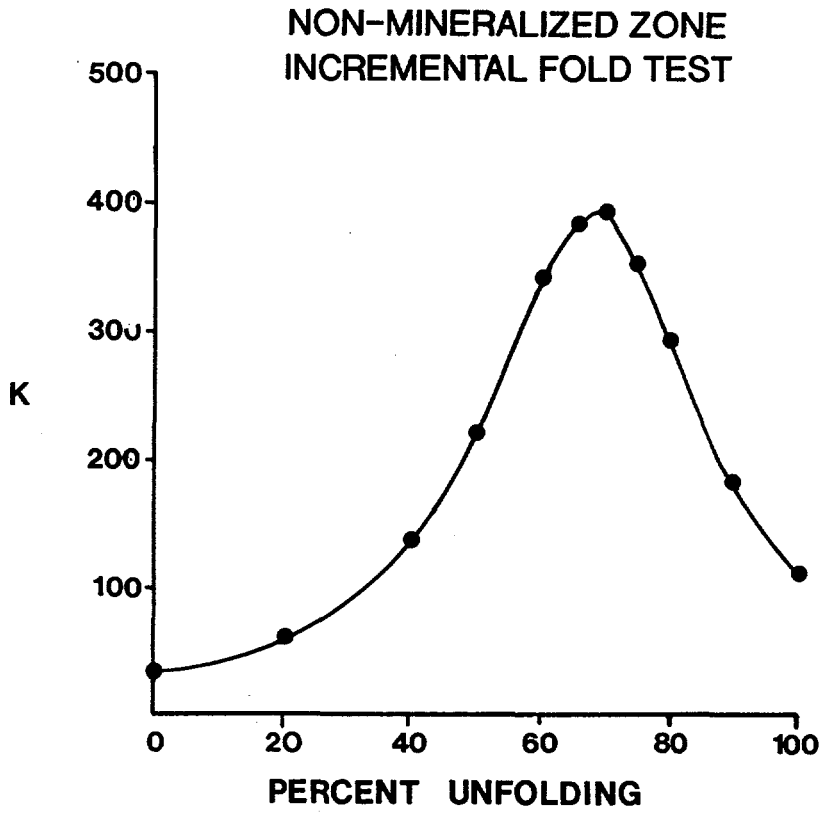

Figure 13. An incremental fold test was performed on the site means from six sample sites from the non-mineralized zone, and it was determined that the best grouping (k) of specimens came at 70% unfolding, indicative of a synfolding magnetization.

Arbuckle Mountain Field Trip
Selected References

Arbuckle Mountains - General

Brown, W.G., R.C. Grayson, Jr., W.H. Jamieson, Jr., J.T. Altum, and J. Hightower, 1985, Tectonism and sedimentation in the Arbuckle Mountain region, southern Oklahoma aulacogen: Waco, Texas, Baylor Geological Society, Baylor University, 44 p.

Fay, R.O., 1988, I-35 roadcuts; geology of Paleozoic strata in the Arbuckle Mountains of southern Oklahoma, in O.T. Hayward, ed., South-Central section: Geological Society of America Centennial Field Guide, v. 4, p. 183-188.

Fay, R.O., 1989, Geology of the Arbuckle Mountains along Interstate 35, Carter and Murray Counties, Oklahoma: Oklahoma Geological Survey Guidebook 26, 50 p.

Ham, W.E., 1969, Regional geology of the Arbuckle Mountains, Oklahoma: Oklahoma Geological Survey Guidebook 17, 52 p.

Ham, W.E., 1973, Regional geology of the Arbuckle Mountains, Oklahoma: Oklahoma Geological Survey Special Publication 73-3, 61 p.

Ham, W.E., M.E. McKinley, and others, 1954 (revised by K.S. Johnson, 1990), Geologic map and sections of the Arbuckle Mountains, Oklahoma: Oklahoma Geological Survey Map GM-31, scale 1:100,000.

Johnson, K.S., M.R. Burchfield, and W.E. Harrison, 1984, Guidebook for Arbuckle Mountain field trip, southern Oklahoma: Oklahoma Geological Survey Special Publication 84-1, 21 p.

Perry, W.J., Jr., 1989, Tectonic evolution of the Anadarko basin region, Oklahoma: U.S. Geological Survey Bulletin 1866-A, 19 p.

Woodford Shale - General

Amsden, T.W., 1960, Stratigraphy and paleontology of the Hunton Group in the Arbuckle Mountain region, part 6: Hunton stratigraphy: Oklahoma Geological Survey Bulletin 84, 311 p. (Woodford, p. 135-140).

Cardott, B.J., 1989, Thermal maturation of the Woodford Shale in the Anadarko basin, in K.S. Johnson, ed., Anadarko basin symposium, 1988: Oklahoma Geological Survey Circular 90, p. 32-46.

Cardott, B.J., W.J. Metcalf, III, and J.L. Ahern, 1990, Thermal maturation by vitrinite reflectance of Woodford Shale near Washita Valley fault, Arbuckle Mountains, Oklahoma, in V.F. Nuccio and C.E. Barker, eds., Applications of thermal maturity studies to energy exploration: S.E.P.M. Rocky Mountain Section, p. 139-146.

Comer, J.B., and H.H. Hinch, 1987, Recognizing and quantifying expulsion of oil from the Woodford Formation and age-equivalent rocks in Oklahoma and Arkansas: American Association of Petroleum Geologists Bulletin, v. 71, p. 844-858.

Jones, P.J., 1986, The petroleum geochemistry of the Pauls Valley area, Anadarko basin, Oklahoma: Norman, University of Oklahoma, unpublished M.S. thesis, 175 p.

Philp, R.P., P.J. Jones, L.H. Lin, G.E. Michael, and C.A. Lewis, 1989, An organic geochemical study of oils, source rocks, and tar sands in the Ardmore and Anadarko basins, in K.S. Johnson, ed., Anadarko basin symposium, 1988: Oklahoma Geological Survey Circular 90, p. 65-76.

Philp, R.P., J. Chen, A. Galvez-Sinibaldi, H. Wang, and J.D. Allen, in press, The effects of weathering and maturity on the geochemical characteristics of the Woodford Shale, in K.S. Johnson and B.J. Cardott, eds., Source rocks in the southern Midcontinent, 1990 symposium: Oklahoma Geological Survey Circular 93.

Taff, J.A., 1902, Description of the Atoka quadrangle: U.S. Geological Survey, Atoka folio 79, 8 p.

Urban, J.B., 1960, Microfossils of the Woodford Shale (Devonian) of Oklahoma: Norman, University of Oklahoma, unpublished M.S. thesis, 77 p.

Von Almen, W.F., 1970, Palynomorphs of the Woodford Shale of south central Oklahoma with observations on their significance in zonation and paleoecology: Michigan State University, unpublished Ph.D. dissertation, 179 p.

Zemmels, I., and C.C. Walters, 1987, Variation of oil composition in vicinity of Arbuckle Mountains, Oklahoma (abstract): American Association of Petroleum Geologists Bulletin, v. 71, p. 998-999.

Woodford Shale - Stop 2 (I-35 roadcut)

Barrick, J.E., and G. Klapper, 1990, Henryhouse and Haragan Formations (Late Silurian-Early Devonian) and Woodford Shale (Late Devonian-Early Mississippian), in S.M. Ritter, ed., Early to middle Paleozoic conodont biostratigraphy of the Arbuckle Mountains, southern Oklahoma: Oklahoma Geological Survey Guidebook 27, p. 11-13.

Brown, W.G., and others, 1985, Stop 6 - The Hunton, Woodford and Sycamore Formations, p. 20-22.

Kirkland, D.W., R.E. Denison, D.M. Summers, and J.R. Gormly, in press, Geology and organic geochemistry of the Woodford Shale in the Criner Hills and western Arbuckle Mountains, Oklahoma, in K.S. Johnson and B.J. Cardott, eds., Source rocks in the southern Midcontinent, 1990 symposium: Oklahoma Geological Survey Circular 93.

Lewan, M.D., 1983, Effects of thermal maturation on stable organic carbon isotopes as determined by hydrous pyrolysis of Woodford Shale: Geochimica et Cosmochimica Acta, v. 47, p. 1471-1479.

Lewan, M.D., 1985, Evaluation of petroleum generation by hydrous pyrolysis experimentation: Philosophical Transactions of the Royal Society of London, series A, v. 315, p. 123-134.

Lewan, M.D., 1987, Petrographic study of primary petroleum migration in the Woodford Shale and related rock units, in B. Doligez, ed.,

Migration of hydrocarbons in sedimentary basins: Paris, Editions Technip, Collection Colloques et Seminaires, p. 113-130.
Roberts, C.T., and R.M. Mitterer, in press, Laminated black shale-bedded chert cyclicity in the Woodford Formation, southern Oklahoma, in K.S. Johnson and B.J. Cardott, eds., Source rocks in the southern Midcontinent, 1990 symposium: Oklahoma Geological Survey Circular 93.
TSOP, 1989, Influence of kerogen isolation methods on petrographic and bulk chemical composition of a Woodford Shale sample: The Society for Organic Petrology, subcommittee report, 35 p.

Stop 3 - Hunton Quarry

Brown, W.G., and others, 1985, Stop 8 - Structures in the Hunton quarry, p. 26-27.
Chaplin, J.R., 1989, Guidebook for selected geologic stops in the Arbuckle Mountains: Oklahoma Geological Survey, prepared for AASG annual meeting, Stop 5 - Hunton anticline and Hunton quarry, p. 50-56.
Hycrude Corporation, 1986, Beneficiation-hydroretorting of U.S. oil shales: University of Alabama, Mineral Resources Institute, Woodford Shale, p. 6, 7, B-7, C-7.
Johnson, K.S., and others, 1984, Stop 4 - Hunton limestone quarry and Woodford oil-shale pit, p. 18-20.

Asphalt deposits - general

Brown, W.G., and others, 1985, Stop 6, Day 2 - The Vanoss conglomerate and Oil Creek sandstone, p. 40-41.
Chaplin, J.R., 1989, Stop 4 - Buckhorn asphalt quarry, p. 42-50.
Gorman, J.M., and G.M. Flint, Jr., 1944, Geologic map of the Dougherty asphalt area, Murray County, Oklahoma: U.S. Geological Survey Oil and Gas Investigations Preliminary Map 15, scale 1 in. = 300 ft.
Ham, W.E., 1950, Guidebook of field trip in the Arbuckle Mountains for Industrial Minerals Division A.I.M.E.: Oklahoma Geological Survey, 30 p.
Harrison, W.E., and M.R. Burchfield, 1983, Tar-sand potential of selected areas in Carter and Murray Counties, south-central Oklahoma: U.S. Department of Energy, Contract DE-AS20-8ILC10730, 221 p.
Harrison, W.E., and M.R. Burchfield, 1987, Resource evaluation of selected tar-sand deposits in southern Oklahoma, in R.F. Meyer, ed., Exploration for heavy crude oil and natural bitumen: American Association of Petroleum Geologists Studies in Geology 25, p. 571-588.
Heaney, M.J., and T.E. Yancey, 1991, Exceptional preservation of bivalved molluscs in the Buckhorn asphalt deposit (Pennsylvanian) of Oklahoma (abstract): Geological Society of America, abstracts with programs, v. 23, no. 5, p. A166-A167.
Hutchison, L.L., 1911, Preliminary report on the rock asphalt, asphaltite, petroleum and natural gas in Oklahoma: Oklahoma Geological Survey Bulletin 2, 256 p.

Jordan, L., 1964, Petroleum-impregnated rocks and asphaltite deposits of Oklahoma: Oklahoma Geological Survey Map GM-8, scale 1:750,000.
Lin, L.H., 1987, Effect of biodegradation on tar sand bitumen of south Woodford area, Carter County, Oklahoma: Norman, University of Oklahoma, unpublished M.S. thesis, 91 p.
Lin, L.H., G.E. Michael, G. Kovachev, H. Zhu, R.P. Philp, and C.A. Lewis, 1989, Biodegradation of tar-sand bitumens from the Ardmore and Anadarko basins, Carter County, Oklahoma: Organic Geochemistry, v. 14, p. 511-523.
Michael, G.E., L.H. Lin, R.P. Philp, C.A. Lewis, and P.J. Jones, 1989, Biodegradation of tar-sand bitumens from the Ardmore/Anadarko basins, Oklahoma -- II. Correlation of oils, tar sands and source rocks: Organic Geochemistry, v. 14, p. 619-633.

Stop 4 - Sulphur Asphalt Deposit

Johnson, K.S., and others, 1984, Stop 3 - Tar sands of Sulphur area, p. 16-18.
Williams, D.B., 1983, Structural and geochemical study of the south Sulphur asphalt deposits, Murray County, Oklahoma: Norman, University of Oklahoma, unpublished M.S. thesis, 163 p.
Williams, D.B., 1986, Structural and geochemical study of the south Sulphur asphalt deposits, Murray County, Oklahoma: Oklahoma City Geological Society, Shale Shaker, v. 36, p. 182-196.

LAMINATED BLACK SHALE-BEDDED CHERT CYCLICITY IN THE WOODFORD FORMATION, SOUTHERN OKLAHOMA

Charles T. Roberts
ARCO Oil and Gas Co., Plano, Texas

Richard M. Mitterer
University of Texas at Dallas

ABSTRACT.—In southern Oklahoma, the Woodford Formation consists of cyclic deposits of laminated black shales and bedded cherts. Organic carbon ranges from 3 to 9% in cherts and from 10 to 25% in black shales. Pyrolysis-gas chromatography, Rock-Eval and carbon isotopic analyses signify that the Woodford contains marine, oil-prone type II kerogen. Except for the difference in organic carbon content, the kerogens of the bedded chert-black shale couplets are analytically similar. The high organic carbon concentrations and the presence of laminated black shales throughout the entire thickness of the formation in southern Oklahoma indicate that deposition in this region occurred under continuous anoxic conditions. The cyclicity exhibited by the couplets represents pulses of high siliceous productivity superimposed on continuous deposition of black shales and may have been caused by external orbital forcing (Milankovitch Cycles).

INTRODUCTION

The Woodford Formation, a Late Devonian–Early Mississippian (Frasnian–Tournaisian) siliceous black shale, is an important hydrocarbon-source rock in the southern Midcontinent region of the United States. The formation is, in part, stratigraphically equivalent to several other organic carbon-rich shales, including the Antrim, Bakken, Chattanooga, New Albany, and Ohio, that together indicate the presence of widespread anoxic conditions over the North American craton during this time.

The organic geochemistry of the Woodford has been studied extensively, and much of the oil produced in central and southern Oklahoma has been correlated with bitumen from the formation (Cardott and Lambert, 1985; Comer and Hinch, 1987). Shales and cherts in the formation contain type II, oil-prone, kerogen with a range of thermal maturities from marginally mature in outcrop areas to metamorphic in the deeply buried portion of the Anadarko basin (Cardott and Lambert, 1985; Houseknecht and Matthews, 1985).

The Woodford Formation occurs in the subsurface over an extensive part of the southern Midcontinent and outcrops in the Arbuckle–Ouachita region of southern Oklahoma and western Arkansas. Lithologically, the formation consists predominantly of black shales in the west, becoming more siliceous eastward (Cardott and Lambert, 1985). In the Arbuckle uplift, cherts and black shales are rhythmically interbedded throughout the formation.

The Woodford is ~91 m thick where it is partially exposed in a road cut (I-35) on the south flank of the Arbuckle uplift, Carter County, Oklahoma. The basal 2–3 m of the formation, immedi-

ately above the unconformity marking the top of the Hunton Group, consist of thinly bedded alternating shales and cherts. The following 67 m is dissected by creek drainage and is extensively covered by vegetation. The almost continuously exposed upper 22 m of Woodford, comprised of alternating beds of organic carbon-rich shales and cherts, constitute the focus of this study.

GEOCHEMISTRY

In the study area, Woodford shales are black to blackish-brown, laminated beds ranging from 0.1 to 29 cm thick (average = 3.2 cm). Cherts are black to blackish-brown, blocky, dense, resistant beds ranging from 0.5 to 32 cm thick (average = 3.5 cm). Thicknesses of both lithologies increase within the top 5 m of the formation. The upper part of the Woodford section contains two zones rich in phosphorite nodules. One zone, 2.3 m from the top of the formation, is 4 m thick, and the second, 10.5 m from the top, is 2 m thick. The majority of the phosphorite nodules are found in chert beds.

A significant amount of poorly preserved radiolarian tests and megaspores are associated with cherts, most notably in phosphate nodules present in the cherts. Microfossils are not observed in the shales. The abundance of siliceous microfossils associated with the cherts indicates that these beds are primary in origin and are not formed as a result of diagenetic processes.

Laminated black shales are highly enriched in organic carbon (C_{org}) with concentrations ranging from 10 to 25% (mean = 13.7%). C_{org} in cherts ranges from about 3 to 9% with a mean of 5.4%. Total sulfur in the shales varies from 0.4 to 4.9% (mean = 1.6%). Total sulfur in the cherts ranges from 0 to 1.0% with a mean of 0.5%. Variations in C_{org} and sulfur correlate entirely with lithology, with shales having more and cherts having less of both elements (Fig. 1). Comer and Hinch (1987) suggested that cherts of the Woodford are deficient in C_{org} relative to the laminated shales because cherts: (1) had higher initial concentrations of biogenic silica (i.e., C_{org} was diluted), (2) were cemented with silica soon after deposition, and (3) underwent little compaction.

A plot of C_{org} and sulfur from Woodford chert and shale samples displays a positive correlation with an approximate zero intercept (Fig. 2). Although both C_{org} and S concentrations in black shales are higher than in cherts, the S/C values for both lithologies fall on the same general trend. The average S/C ratio for all Woodford samples is 0.11. For shales, S/C is 0.12, while for cherts this ratio is 0.09. Thus, S/C is virtually identical in both shales and cherts. For comparison, the average S/C value for normal marine Holocene sediments is 0.36, and for normal marine (i.e., bioturbated) Phanerozoic shales the average S/C is 0.40 (Berner, 1982; Berner and Raiswell, 1983). The results for the Woodford also differ from S/C values obtained from coeval Devonian shales of the Appalachian basin; the latter have a positive S-axis intercept for the S/C trend and have S/C ratios greater than 0.40 (Leventhal, 1987).

The low S/C values for the Woodford samples indicate either that pyrite formation in the depositional environment was limited or that S/C values have been altered subsequent to deposition

and do not represent original concentrations. Post-depositional changes, such as a decrease of organic carbon due to hydrocarbon generation or weathering of pyrite and oxidation of sulfur to more soluble sulfate salts, cannot account for the S/C trend as they would either lead to an increase in the S/C values or cause the data to be more randomly scattered.

Pyrite formation is generally limited by deficiencies in organic carbon, sulfate, or reactive iron (Berner, 1982). High concentrations in both shales and cherts show that organic carbon was not a limiting factor in Woodford sediments. With deposition of Woodford sediments occurring in a marine basin, sulfate also was not limiting. Consequently, the most likely factor limiting pyrite formation in the Woodford was a low content of reactive iron transported to the basin. This inference is supported by the low iron content of Woodford samples (shale—1.5 wt % Fe; chert—0.4 wt % Fe) compared to coeval Chattanooga Shale (6.9 wt % Fe) (Brownlow, 1979) and to Cretaceous Mowry and Pierre Shales of the Western Interior Seaway (about 2–4 wt % Fe) (Dean and Arthur, 1989). Furthermore, the data for the Woodford samples fall on the constant S/Fe line for pyrite (S/Fe = 1.15), representing an iron-limited system, in the Fe–S–OC ternary diagram (Fig. 3). Thus, there is essentially no reactive iron remaining after pyrite formation and the degree of pyritization is virtually 100%. Iron was probably delivered to the sediments as a metal-organic matter complex, accounting for the linear trend in S/C values (Raiswell and Berner, 1985).

Rock-Eval pyrolysis data for 30 shale and chert samples, plotted as hydrogen index (HI) and oxygen index (OI), fall along a vertical trend in the intermediate hydrogen index range (Fig. 4). This trend represents the maturation pathways for types I and II kerogen (Tissot and others, 1974). Shales and cherts show considerable overlap in the type II region. Mean values for the production index and T_{max} for both shale and chert samples are 0.028° and 431°C, respectively. Conclusions drawn from the Rock-Eval data are that the Woodford cherts and shales from the outcrop region examined in this study contain marine, type II, oil-prone kerogen, that they exhibit a submature to slightly mature level of thermal maturation, and that, in general, they show a high degree of genetic source-rock potential.

Carbon-isotope analyses of several samples from the middle of the study interval further characterize the nature of organic matter in the cherts and shales. The mean $\delta^{13}C$ value of Woodford kerogen for both cherts and shales is –29.8‰ (Fig. 1). Isotopic values range from –29.5 to –30.0‰, with no difference in $\delta^{13}C$ values for the kerogens of the two lithologies. The mean isotopic value falls within the general range of marine kerogens of Devonian age (Maynard, 1981).

Despite the differences in C_{org} content, Rock-Eval and carbon isotopic data indicate that shales and cherts contain essentially the same kind of kerogen. Lower organic carbon content of the cherts is inferred to be due to sedimentary dilution of organic matter during periods of high siliceous productivity rather than to differences in type of organic matter.

DEPOSITIONAL MODEL

The Woodford Formation accumulated in a shallow to deep, euxinic epicontinental sea on the southern margin of the North American craton. Deeper portions of the sea existed within the southern Oklahoma aulacogen, which includes the study site. The euxinic environment was favorable for accumulation and preservation of large amounts of organic carbon, as evidenced by the high concentrations in both cherts and shales. Although both lithologies have enhanced organic carbon, the shales are far more enriched than cherts.

Lower concentrations of C_{org} in cherts are inferred to be due to dilution by syngenetically deposited biogenic silica. Cherts were deposited during relatively short periods of high siliceous productivity as organic carbon-rich siliceous oozes. In contrast, shale deposition occurred over a longer interval of time with lower levels of siliceous productivity and less dilution of organic carbon by siliceous sediments. Figure 5 is a model illustrating the two alternating phases of sedimentation.

Relative rates of deposition of chert and shale can be estimated from elemental abundance data. Carbon, nitrogen, and phosphorus are derived almost exclusively from organic matter; consequently, the relative proportion of these constituents in shales and cherts is a measure of the dilution factor due to biogenic silica sedimentation. The shale-to-chert ratio for each of these elements, based on their average concentrations, is 2.5 (Fig. 1). That is, due to dilution by biogenic silica, cherts contain 0.4 times the concentration of C_{org}, N and P that is present in shales. Accordingly, cherts accumulated at least 2.5 times faster than shales. The dilution factor, however, may have been even greater than 2.5 if carbon accumulation rates were higher during chert deposition due to greater productivity at this time.

The time represented by a single chert-shale couplet can only be estimated because of the uncertainty in age range of the Woodford. Deposition of the Woodford lasted from Frasnian (Late Devonian) into Tournaisian (earliest Mississippian) time (Hass and Huddle, 1965; Ham, 1973). There is uncertainty as to how much of the Frasnian and Tournaisian is represented in this section because of the virtual absence of fossils except for poorly preserved radiolarians and conodonts. The Devonian–Mississippian boundary occurs between 4 and 5 m from the top of the formation (Hass and Huddle, 1965), so only a portion of the Tournaisian may be represented. Thus, the time span for Woodford deposition can be estimated minimally and maximally between 10 and 15 Myr.

Based on the average couplet thickness of 6.7 cm and an overall formation thickness of 91 m, individual couplets are estimated to have accumulated in 7.4–11.0 Kyr. Lower frequency periodicities of about 15–21 Kyr and 90–125 Kyr, representing megacycles of two and 10 couplets, are obtained from time series analysis of bedding thicknesses assuming depositional time spans of 10 and 15 Myr. Within the limits of age uncertainty of Woodford deposition, the shale-chert rhythmic periodicities in the Woodford fall within the frequency bands of Milankovitch orbital parameters.

SUMMARY

The Woodford Formation accumulated in a shallow to deep, euxinic epicontinental sea proximal to the southern margin of the North American craton. The euxinic environment was favorable for accumulation and preservation of large amounts of organic matter, as evidenced by the very high organic carbon values in chert and shale lithologies. Although differences exist in the organic carbon concentrations between shales and cherts, the kerogens of the chert-shale couplets are analytically the same (oil-prone type II). The lower organic carbon concentrations in cherts are considered to be due to dilution by syngenetically deposited biogenic silica. Cherts were most likely deposited during relatively short periods of siliceous productivity as organic carbon-rich siliceous oozes. In contrast, shale deposition probably occurred over a longer period of time during lower levels of siliceous productivity and less dilution of organic matter. Ultimate control over the depositional cycles of the Woodford Formation was probably by astronomical (Milankovitch) forcing.

REFERENCES

Berner, R. A., 1982, Burial of organic carbon and pyrite sulfur in the modern ocean: its geochemical and environmental significance: American Journal of Science, v. 282, p. 451–473.

Berner, R. A.; and Raiswell, R., 1983, Burial of organic carbon and pyrite sulfur in sediments over Phanerozoic time: a new theory: Geochimica et Cosmochimica Acta, v. 47, p. 855–862.

Brownlow, A. H., 1979, Geochemistry: Prentice-Hall, Englewood Cliffs, New Jersey, 498 p.

Cardott, B. J.; and Lambert, M. W., 1985, Thermal maturation by vitrinite reflectance of Woodford Shale, Anadarko basin, Oklahoma: American Association of Petroleum Geologists Bulletin, v. 69, p. 1982–1998.

Comer, J. B.; and Hinch, H. H., 1987, Recognizing and quantifying expulsion of oil from the Woodford Formation and age-equivalent rocks in Oklahoma and Arkansas: American Association of Petroleum Geologists Bulletin, v. 71, p. 844–858.

Dean, W. E.; and Arthur, M. A., 1989, Iron-sulfur-carbon relationships in organic carbon-rich sequences I: Cretaceous Western Interior Seaway: American Journal of Science, v. 289, p. 708–743.

Ham, W. E., 1973, Regional geology of the Arbuckle Mountains, Oklahoma: Oklahoma Geological Survey Special Publication 73-3, 61 p.

Hass, W. H.; and Huddle, J. W., 1965, Late Devonian and Early Mississippian age of the Woodford Shale in Oklahoma, as determined by conodonts: U.S. Geological Survey Professional Paper 525-D, p. 125–132.

Houseknecht, D. W.; and Matthews, S. M., 1985, Thermal maturity of Carboniferous strata: American Association of Petroleum Geologists Bulletin, v. 69, p. 335–345.

Leventhal, J. S., 1987, Carbon and sulfur relationships in Devonian shales from the Appalachian basin as an indicator of environment of deposition: American Journal of Science, v. 287, p. 33–49.

Maynard, J. B., 1981, Carbon isotopes as indicators of dispersal patterns in Devonian–Mississippian shales of the Appalachian basin: Geology, v. 9, p. 262–265.

Raiswell, R.; and Berner, R. A., 1985, Pyrite formation in euxinic and semi-euxinic sediments: American Journal of Science, v. 285, p. 710–724.

Tissot, B.; Durand, B.; Espitalié, J.; and Combaz, A., 1974, Influence of nature and diagenesis of organic matter in petroleum formation: American Association of Petroleum Geologists Bulletin, v. 58, p. 499–506.

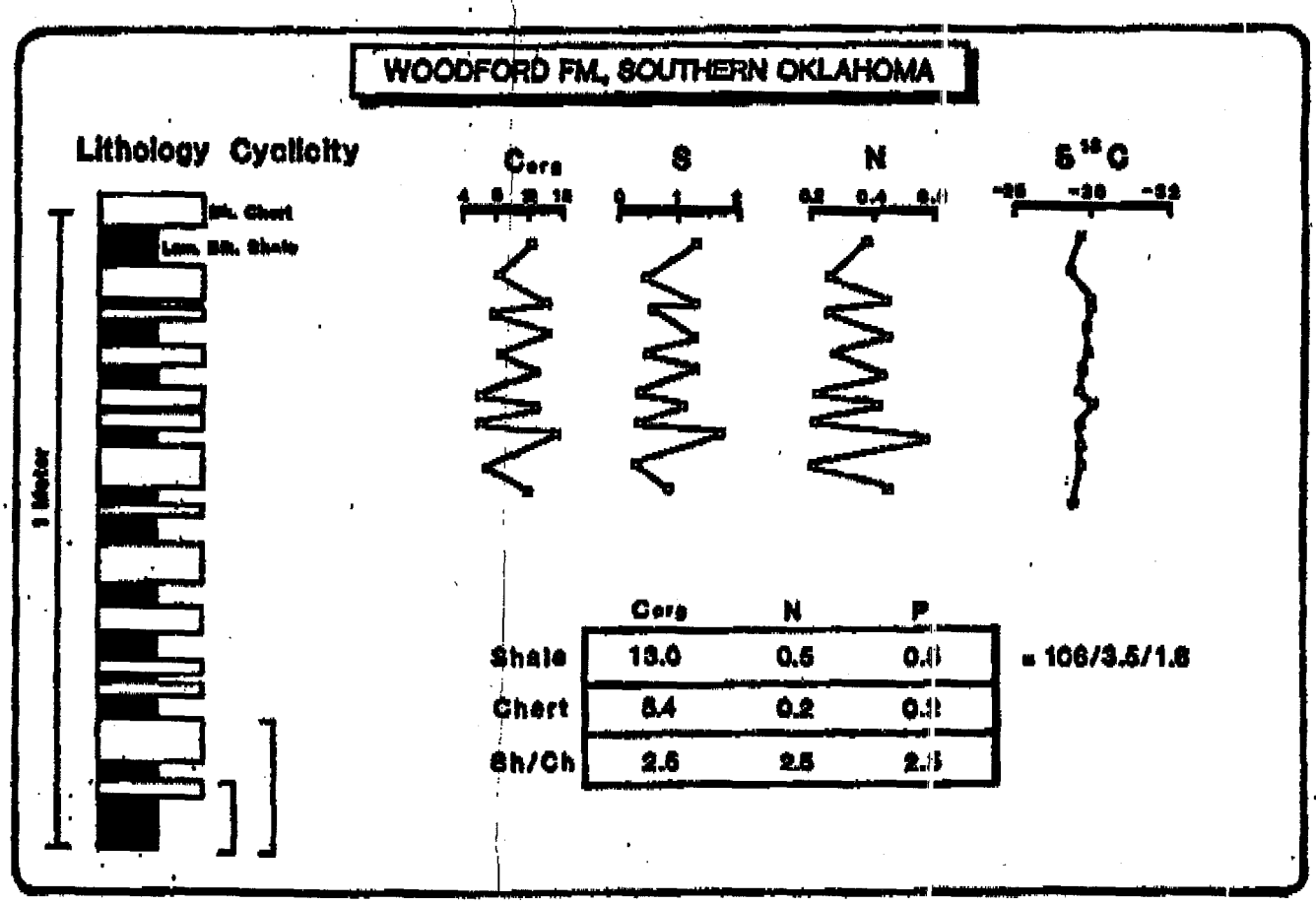

Figure 1. A schematic diagram of a 1-m section of the Woodford Formation at its outcrop on the southern flank of the Arbuckle uplift, Interstate 35, Carter County, Oklahoma illustrating the rhythmic deposition of laminated black shale and chert. Variations in organic carbon, total sulfur, total nitrogen, and carbon isotopic composition of kerogen are plotted for a portion of this section. Average carbon, nitrogen, and phosphorus concentrations for shales and cherts are indicated in the box at bottom.

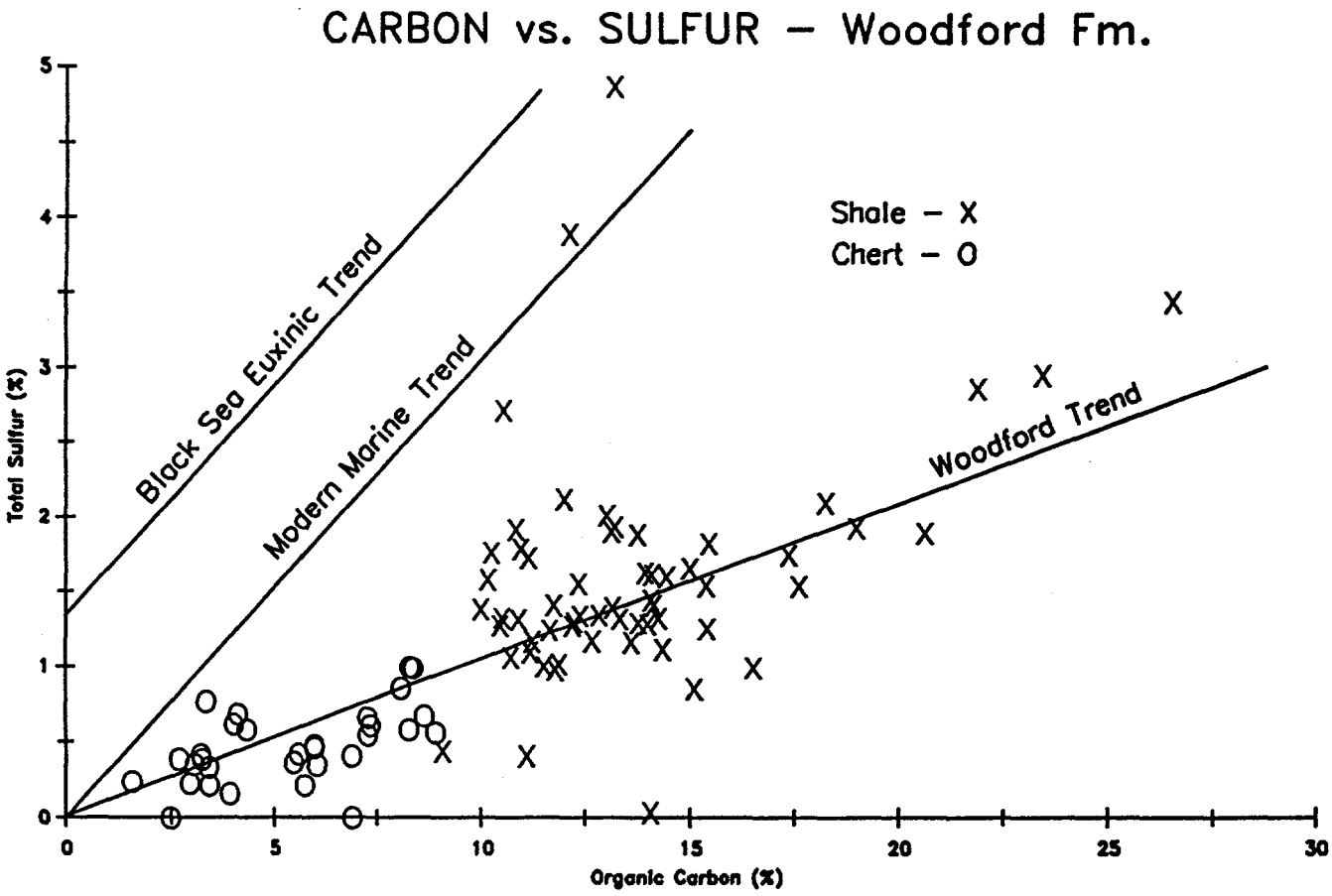

Figure 2. Organic carbon vs. total sulfur for chert and shale samples of the Woodford Formation compared to trends obtained for normal marine (Berner and Raiswell, 1983) and Black Sea (Leventhal, 1983) sediment samples.

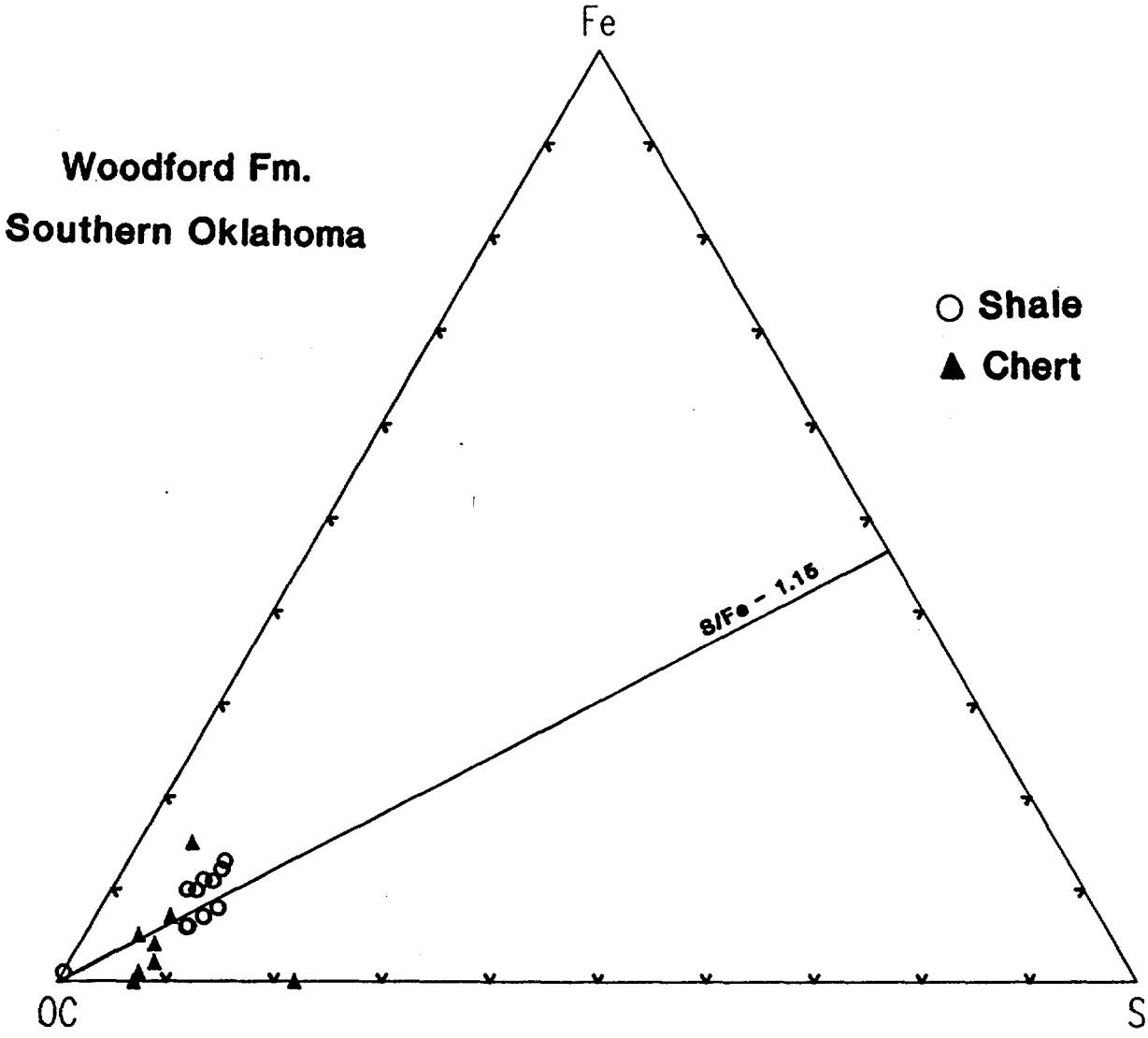

Figure 3. Fe–S–OC ternary diagram for samples of the Woodford Formation. The line represents the constant value for the ratio (by weight) of sulfur-to-iron in pyrite (S/Fe = 1.15). Samples falling on this line are inferred to have been deposited in an iron-limited system.

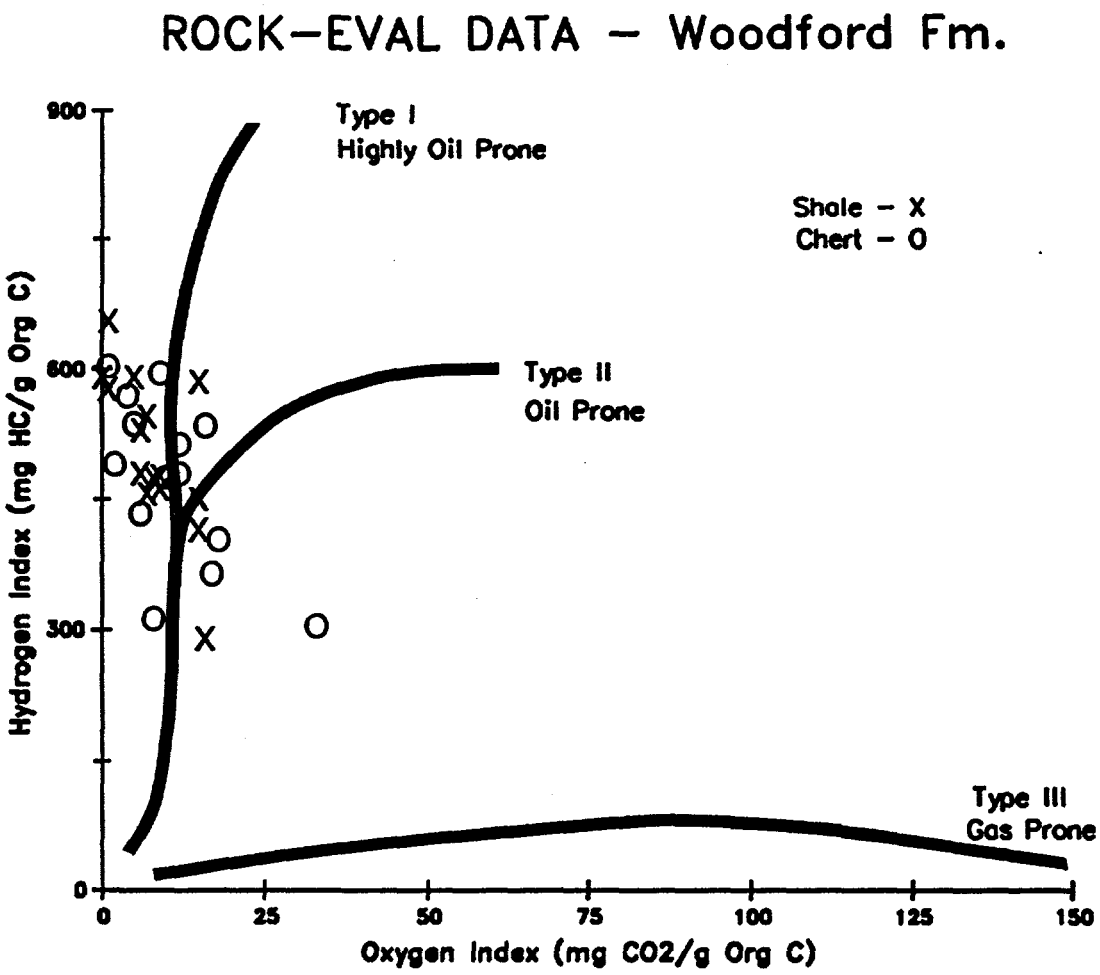

Figure 4. Rock-Eval hydrogen index (HI) vs. oxygen index (OI) for 30 whole rock chert and shale samples of the Woodford Formation.

Southern Oklahoma Aulacogen - Cyclic Sedimentation

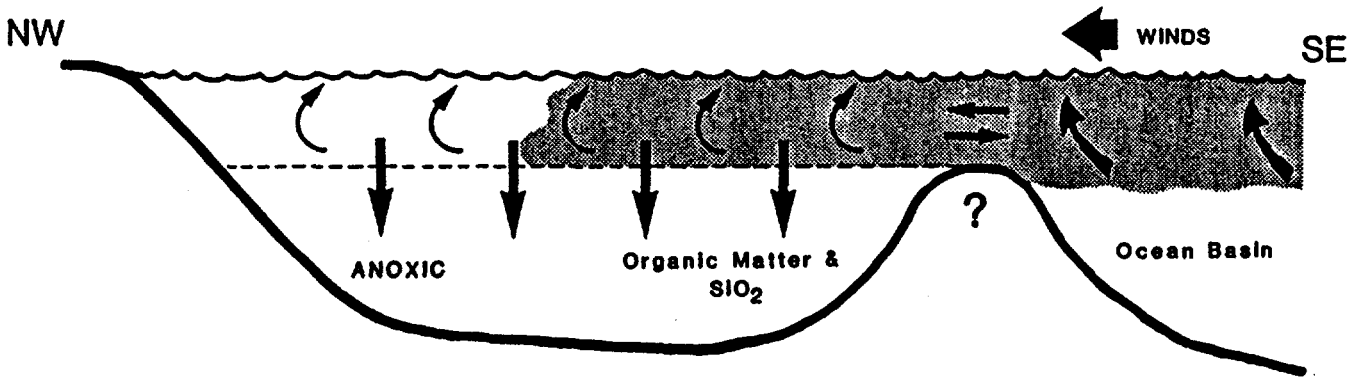

(A) Intensification of wind & upwelling currents, high organic & siliceous productivity, chert deposition.

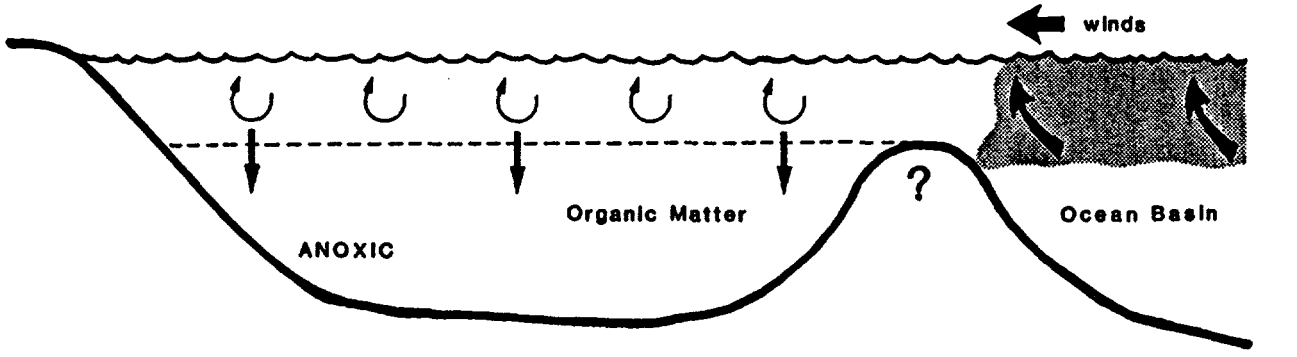

(B) Decrease in intensity of wind & upwelling currents, lower organic productivity, black shale deposition.

Zooplanktonic siliceous productivity

Figure 5. Depositional model for the Woodford Formation in the southern Oklahoma aulacogen.

Reprint removed
Jacobs 3-3-97